

SLAM Backends with Objects in Motion: A Unifying Framework and Tutorial

Chih-Yuan Chiu*

Abstract—Simultaneous Localization and Mapping (SLAM) algorithms are frequently deployed to support a wide range of robotics applications, such as autonomous navigation in unknown environments, and scene mapping in virtual reality. Many of these applications require autonomous agents to perform SLAM in highly dynamic scenes. To this end, this tutorial extends a recently introduced, unifying optimization-based SLAM backend framework to environments with moving objects and features [1]. Using this framework, we consider a rapprochement of recent advances in dynamic SLAM. Moreover, we present *dynamic EKF SLAM*, a novel, filtering-based dynamic SLAM algorithm generated from our framework, and prove that it is mathematically equivalent to a direct extension of the classical EKF SLAM algorithm to the dynamic environment setting. Empirical results with simulated data indicate that dynamic EKF SLAM can achieve high localization and mobile object pose estimation accuracy, as well as high map precision, with high efficiency.

Index Terms—Simultaneous Localization and Mapping, Vision, Dynamics, Estimation.

I. INTRODUCTION

Simultaneous Localization and Mapping (SLAM) is a well-studied robotics problem in which an autonomous agent attempts to locate itself in an uncharted environment while constructing a map of said environment [2, 3]. Most state-of-the-art SLAM algorithms operate under the *static world* setting, in which the locations of landmarks in the robot’s environment are assumed to be fixed. This greatly restricts the applicability of SLAM algorithms to robotics tasks such as autonomous navigation, in which SLAM-constructed maps must describe a wide variety of dynamic objects, such as moving obstacles, human-operated vehicles, or other autonomous agents.

To bridge this gap, the rapidly maturing *dynamic SLAM* community aims to design SLAM algorithms that track moving objects while performing SLAM on the underlying static scene. Specifically, dynamic SLAM algorithms simultaneously estimate *ego robot states*, *static features*, *features on moving objects*, and *poses of moving objects*. To this end, Wang et al. proposed the SLAMMOT algorithm, which separately performs motion tracking for dynamic objects and SLAM over an underlying, fixed background [4]. Yang et al. introduced CubeSLAM, which assigns each dynamic object a rectangular bounding box, and tracks the boxes’ trajectories across time [5]. Huang et al. proposed ClusterSLAM, which aggregates feature points corresponding to various dynamic objects in the scene, then performs bundle adjustment over each cluster [6]. Bescos et al. presented DynaSLAM and DynaSLAM II, which uses the ORB-SLAM algorithm to extract features of,

and subsequently track, dynamic objects [7, 8]. Zhang et al. introduce VDO-SLAM, which fuses dense optical flow and image segmentation to perform joint inference over robot poses, static landmark positions, and the pose and feature positions of mobile objects [9]. Although these approaches obtain reasonable accuracy in tracking moving objects, they typically incur a computational burden that increases rapidly with the number of moving objects tracked, and the length of the time horizon over which inference is performed.

In this work, we extend the unifying, optimization-based SLAM formulation in [1] to the dynamic SLAM setting. We illustrate that the aforementioned dynamic SLAM algorithms employ back-ends corresponding to different design choices in the context of our framework. To address the computational limitations of existing methods, we use our framework to derive *dynamic EKF-SLAM*, a filtering-based algorithm that establishes a rapprochement between two classes of algorithms: efficient conventional filtering-based methods for static-world SLAM [10], and accurate but computationally costly bundle adjustment methods underlying existing dynamic SLAM algorithms. We prove that dynamic EKF SLAM is mathematically equivalent to a straightforward extension of the conventional EKF-SLAM algorithm to dynamic scenes. We then illustrate the empirical success of dynamic EKF-SLAM in performing inference over a simulated driving scenario, in which an ego autonomous vehicle travels down a highway in the presence of two other vehicles and a jaywalking pedestrian.

II. DYNAMIC SLAM: A UNIFYING FRAMEWORK

Suppose that, at time $t \geq 0$, the estimated variables of the ego robot describe its past and/or present poses, $n_f \in \mathbb{N}$ static features, and $n_o \in \mathbb{N}$ moving objects with $n_{of}(\alpha) \in \mathbb{N}$ features for each object index $\alpha \in \{1, \dots, n_o\}$. Given $n, n_1, n_2 \in \mathbb{N}$, with $n_1 < n_2$, set $[n] := \{1, \dots, n\}$ and $[n_1 : n_2] := \{n_1, \dots, n_2\}$. We have:

- $\{x_t \in \mathbb{R}^{d_x} : t \in [T]\}$ denotes ego robot states, e.g., its poses and velocities, etc., relative to a global frame \mathbf{G} .
- $\{f_k^{(s)} \in \mathbb{R}^{d_f} : k \in [n_f]\}$ describes the current position estimate of each of the n_f currently tracked static features relative to frame \mathbf{G} , with corresponding feature measurements $\{z_{t,k}^{(s)} \in \mathbb{R}^{d_z} : t \in \{0\} \cup [T], k \in [n_f]\}$ at each time $t \in \{0\} \cup [T]$.
- $\{f_{t,\alpha,k}^{(m)} \in \mathbb{R}^{d_f} : t \in \{0\} \cup [T], \alpha \in [n_o], k \in [n_{of}(\alpha)]\}$ describes the feature position estimates, at each time $t \in \{0\} \cup [T]$, of each of the k features on the α -th moving object, maintained in the estimation window relative to frame \mathbf{G} , with corresponding feature measurements $\{z_{t,\alpha,k}^{(m)} \in \mathbb{R}^{d_z} : t \in \{0\} \cup [T], \alpha \in [n_o], k \in [n_{of}(\alpha)]\}$.

*Corresponding author. The author is with the EECS Department at the University of California, Berkeley, CA 94720 USA (email: chihyuan_chiu at berkeley dot edu.).

- $\{\xi_{t,\alpha} : t \in [T], \alpha \in [n_o]\}$ describes the poses of each of the n_o currently tracked moving objects at time t relative to its pose at time 0.

The evolution of states, features (associated with both static and moving objects), and moving object poses are captured by the following infinitely continuously differentiable (i.e., C^∞) maps. The ego robot dynamics map $g : \mathbb{R}^{d_x} \rightarrow \mathbb{R}^{d_x}$, the feature measurement map $h : \mathbb{R}^{d_x} \times \mathbb{R}^{d_f} \rightarrow \mathbb{R}^{d_z}$, and the moving object pose transform map $g^o : \mathbb{R}^{d_x} \times \mathbb{R}^{d_x} \rightarrow \mathbb{R}^{d_x}$, are defined via additive noise models as shown below:

$$x_{t+1} = g(x_t) + w_t, \quad w_t \sim \mathcal{N}(0, \Sigma_w), \quad (1)$$

$$z_{t,k} = h(x_t, f_k) + v_{t,k}, \quad v_{t,k} \sim \mathcal{N}(0, \Sigma_v), \quad (2)$$

$$f_{t,\alpha,k}^{(m)} = g^o(\xi_{t,\alpha}, f_{0,\alpha,k}^{(m)}) + n_{t,\alpha}, \quad n_{t,\alpha} \sim \mathcal{N}(0, \Sigma_\xi), \quad (3)$$

$$\forall t \in \{0\} \cup [T], \alpha \in [n_o], k \in [n_{of}(\alpha)].$$

where $\mathcal{N}(\mu, \Sigma)$ denotes the Gaussian distribution with mean $\mu \in \mathbb{R}^d$ and covariance matrix $\Sigma \in \mathbb{R}^{d \times d}$, for some $d \in \mathbb{N}$, and $\Sigma_w \in \mathbb{R}^{d_x \times d_x}$, $\Sigma_v \in \mathbb{R}^{d_z \times d_z}$, $\Sigma_\xi \in \mathbb{R}^{d_x \times d_x}$ are symmetric positive definite (p.d.) noise covariances. In the sections below, we assume that $\frac{\partial h}{\partial f_k}(x_t, f_k)$ is surjective at each $(x_t, f_k) \in \mathbb{R}^{d_x} \times \mathbb{R}^{d_f}$, and that $\frac{\partial g^o}{\partial \xi_{t,\alpha}}$ is injective at each $(\xi_{t,\alpha}, f_{0,\alpha}^{(m)}) \in \mathbb{R}^{d_x} \times \mathbb{R}^{d_f}$.

Our optimization-based formulation of dynamic SLAM includes the following steps, each of which updates the running cost term (“cost \rightarrow cost’’).

1) Feature Augmentation:

Let $\{z_k : k \in I_f\} \subset \mathbb{R}^{d_z}$ denote feature measurements, taken with respect to previously untracked features $\{f_k : k \in I_f\} \subset \mathbb{R}^{d_f}$. These may correspond to static or moving objects. The *feature augmentation* step updates the running cost to include residual terms concerning these newly observed features:

$$\text{cost}' = \text{cost} + \sum_{k \in I_f} \|z_{t,k} - h(x_t, f_k)\|_{\Sigma_v^{-1}}^2$$

2) Moving Object Pose Augmentation:

Let $\{f_{t,\alpha,k}^{(m)} : k \in I_{f,\alpha}, \alpha \in I_o\}$ denote features of tracked moving objects that have been observed at times t_1 and t_2 , with $t_1 < t_2$. For simplicity, define:

$$f_{\tau,\alpha}^{(m)} := (f_{\tau,\alpha,1}^{(m)}, \dots, f_{\tau,\alpha,n_{of}(\alpha)}^{(m)}) \in \mathbb{R}^{n_{of}(\alpha)d_f},$$

for each $\alpha \in [n_o]$, $\tau \in \{0, t\}$. The *moving object pose augmentation* step appends the current pose estimates of tracked moving objects, i.e., $\{\xi_{t,\alpha} : \alpha \in [n_o]\}$, to the running cost:

$$\text{cost}' = \text{cost} + \sum_{\alpha \in I_o} \sum_{k \in I_{f,\alpha}} \|f_{t,\alpha,k}^{(m)} - g^o(\xi_{t,\alpha}, f_{0,\alpha,k}^{(m)})\|_{\Sigma_\xi^{-1}}^2$$

3) Static Feature Update:

Let $\{z_k : k \in I_f\} \subset \mathbb{R}^{d_z}$ denote feature measurements, taken with respect to previously tracked static features $\{f_k^{(s)} : k \in I_f\} \subset \mathbb{R}^{d_f}$. The *feature update* step updates the cost as follows:

$$\text{cost}' = \text{cost} + \sum_{k \in I_f} \|z_{t,k}^{(s)} - h(x_t, f_k^{(s)})\|_{\Sigma_v^{-1}}^2$$

4) Smoothing Factor Augmentation:

The *smoothing factor augmentation* step constrains the most recent moving object pose transformation ($\xi_{t-1,\alpha}$ to $\xi_{t,\alpha}$) from significantly differing from the second most recent moving object pose transformation ($\xi_{t-2,\alpha}$ to $\xi_{t-1,\alpha}$), for each object indexed $\alpha \in [n_o]$:

$$\text{cost}' = \text{cost} + \sum_{\alpha \in I_o} \|s(\xi_{t-2,\alpha}, \xi_{t-1,\alpha}, \xi_{t,\alpha})\|_{\Sigma_s^{-1}}^2$$

Here, $s : \mathbb{R}^{3d_x} \rightarrow \mathbb{R}^{d_x}$ is a smoothing function, e.g., for $d_x = 1$, take $s(\xi_{t-2,\alpha}, \xi_{t-1,\alpha}, \xi_{t,\alpha}) := (\xi_{t,\alpha} - \xi_{t-1,\alpha}) - (\xi_{t-1,\alpha} - \xi_{t-2,\alpha})$.

5) State Propagation:

At each time t , the *state propagation step* updates the cost to include residual terms involving the odometry measurements between x_t , the pose at time t , and x_{t+1} , the pose at time $t+1$:

$$\text{cost}' = \text{cost} + \|x_{t+1} - g(x_t)\|_{\Sigma_w^{-1}}^2$$

Poses and features present in the optimization window may be dropped (instead of marginalized) to improve optimization accuracy, as is common in SLAM algorithms operating under the static world assumption [11, 12]. In addition, the above formulation naturally extends to scenarios in which dynamical quantities evolve on smooth manifolds, rather than on Euclidean spaces (see [1], Section 3 and Appendix A).

III. UNIFYING EXISTING ALGORITHMS

In this section, we interpret the back-ends of recently proposed dynamic SLAM algorithms as the selection of different design choices within the context of our framework, as presented in Section II. We focus in particular on design choices relevant to tracking moving objects.

- **CubeSLAM** [5]—In CubeSLAM, pose estimates of moving objects are obtained by forming and tracking rectangular bounding boxes across time. Feature augmentation of moving objects into the estimation window is avoided.
- **ClusterSLAM** [6]—ClusterSLAM models moving objects by aggregating and tracking feature clouds. The authors describe “fully-coupled”, “semi-decoupled”, and “decoupled” estimation schemes for static SLAM and moving object tracking, which correspond to increasingly aggressive marginalization schemes in our framework.
- **VDO-SLAM** [9]—The VDO-SLAM algorithm performs object segmentation, then samples dense feature clouds within each bounding box to track the associated moving object. In contrast with CubeSLAM, this is a vigorous feature and pose augmentation scheme, with little marginalization within the estimation window. VDO-SLAM can enjoy considerable accuracy, but may also incur high computational burden [8].
- **DynaSLAM II** [8]—DynaSLAM II tracks moving objects across time, by repeatedly performing pose augmentation with pose estimates constructed from newly observed features. Unlike VDO-SLAM, the most recent feature position estimates of these moving objects are then quickly dropped or marginalized, to reduce the computation burden at the next timestep.

Algorithm 1: Dynamic EKF SLAM, as Iterative optimization.

Data: Prior $\mathcal{N}(\mu_0, \Sigma_0)$ on $x_0 \in \mathbb{R}^{d_x}$, noise covariances $\Sigma_w \in \mathbb{R}^{d_x \times d_x}$, $\Sigma_v \in \mathbb{R}^{d_z \times d_z}$, $\Sigma_\xi \in \mathbb{R}^{d_x \times d_x}$, $\Sigma_s \in \mathbb{R}^{d_x \times d_x}$, dynamics map $g : \mathbb{R}^{d_x} \times \mathbb{R}^{d_x}$, measurement map $h : \mathbb{R}^{d_x} \times \mathbb{R}^{d_f} \times \mathbb{R}^{d_z}$, inverse measurement map $\ell : \mathbb{R}^{d_x} \times \mathbb{R}^{d_z} \times \mathbb{R}^{d_f}$, moving object dynamics map $g_o^\alpha : \mathbb{R}^{d_x} \times \mathbb{R}^{n_{of}(\alpha)d_f} \times \mathbb{R}^{n_{of}(\alpha)d_f}$ for each object indexed $\alpha \in [n_o]$, inverse moving object dynamics map $\gamma : \mathbb{R}^{n_{of}(\alpha)d_f} \times \mathbb{R}^{n_{of}(\alpha)d_f} \rightarrow \mathbb{R}^{d_x}$, time horizon $T \in \mathbb{N}$, number of features $n_f \in \mathbb{N}$, number of moving objects $n_o \in \mathbb{N}$.

Result: Estimates $\mu_t, \forall t \in \{1, \dots, T\}$.

```

1  $\text{cost}_0 \leftarrow \|x_0 - \mu_0\|_{\Sigma_0^{-1}}^2$ 
2  $n_f, n_o \leftarrow 0$ .
3 for  $t = 0, 1, \dots, T-1$  do
4    $n_f \leftarrow$  Number of tracked features on static features
5    $N_f \leftarrow$  Total number of tracked features on moving objects
6    $\{z_{t,k} : k \in [n_f + N_f + 1 : n_f + N_f + N'_f]\} \leftarrow$  Measurements of new features, corresponding to both static landmarks and moving objects.
7    $\text{cost}_t \leftarrow$ 
8      $\text{cost}_t + \sum_{k=n_f+N_f+1}^{n_f+N_f+n'_f+N'_f} \|z_{t,k}^{(s)} - h(x_t, f_k^{(s)})\|_{\Sigma_v^{-1}}^2$ .
9    $\mu_t, \Sigma_t \leftarrow$  Gauss-Newton, on  $\text{cost}_t$ , about  $\mu_t$  ([1], Alg. 3).
10  Increment  $n_f, n_o, \{n_{of}(\alpha) : \alpha \in [n_o]\}$  as appropriate, given the newly detected  $n'_f$  static features and  $N'_f$  features on moving objects.
11  if  $n_o \geq 1$  then
12     $\text{cost}_t \leftarrow \text{cost}_t + \sum_{\alpha=1}^{n_o} \sum_{k=1}^{n_{of}(\alpha)} \|f_{t,\alpha,k}^{(m)} - g_o(\xi_{t,\alpha}, f_{t,\alpha,k}^{(m)})\|_{\Sigma_\xi^{-1}}^2 \cdot \mathbf{1}\{f_{t,\alpha,k}^{(m)}, f_{t,\alpha,k}^{(m)} \text{ defined}\}$ .
13     $\mu_t \leftarrow (\mu_t, \gamma(f_{t,1}^{(m)}, f_{t,1}^{(m)}), \dots, \gamma(f_{t,n_o}^{(m)}, f_{t,n_o}^{(m)}))$ .
14     $\mu_t, \Sigma_t \leftarrow$  Gauss-Newton, on  $\text{cost}_t$ , about  $\mu_t$  ([1], Alg. 3).
15    (Optional) Drop  $\{f_{t,\alpha}^{(m)} : \alpha \in [n_o]\}$  from the mean and covariance estimates.
16  end
17   $\text{cost}_t \leftarrow \text{cost}_t + \sum_{\alpha=1}^{n_o} \|s(\xi_{t-2,\alpha}, \xi_{t,\alpha}, \xi_{t,\alpha})\|_{\Sigma_s^{-1}}^2 \cdot \mathbf{1}\{\xi_{t-2,\alpha}, \xi_{t,\alpha}, \xi_{t,\alpha} \text{ defined}\}$ 
18   $\mu_t, \Sigma_t \leftarrow$  Gauss-Newton, on  $\text{cost}_t$ , about  $\mu_t$  ([1], Alg. 3).
19   $\{z_{t,k}^{(s)} : k \in [n_f]\} \leftarrow$  Measurements of existing static features.
20   $\text{cost}_t \leftarrow \text{cost}_t + \sum_{k=1}^{n_f} \|z_{t,k}^{(s)} - h(x_t, f_k^{(s)})\|_{\Sigma_v^{-1}}^2$ .
21   $\bar{\mu}_t, \bar{\Sigma}_t \leftarrow$  Gauss-Newton, on  $\text{cost}_t$ , about  $\mu_t$ , ([1], Alg. 3).
22   $\text{cost}_t \leftarrow \text{cost}_t + \|x_{t+1} - g(x_t)\|_{\Sigma_w^{-1}}^2$ 
23   $\mu_{t+1}, \Sigma_{t+1} \leftarrow$  Marginalization, on  $\text{cost}_{t+1}$  with  $x_M = x_t$ , about  $(\bar{\mu}_t, g(\bar{\mu}_t))$  ([1], Alg. 4).
24   $\text{cost}_{t+1} \leftarrow \|x_{t+1} - \mu_{t+1}\|_{\Sigma_{t+1}^{-1}}^2$ 
25 end
26 return  $\mu_0, \dots, \mu_T$ 

```

Algorithm 2: Dynamic EKF SLAM, Standard formulation.

Data: Prior $\mathcal{N}(\mu_0, \Sigma_0)$ on $x_0 \in \mathbb{R}^{d_x}$, noise covariances $\Sigma_w \in \mathbb{R}^{d_x \times d_x}$, $\Sigma_v \in \mathbb{R}^{d_z \times d_z}$, $\Sigma_\xi \in \mathbb{R}^{d_x \times d_x}$, $\Sigma_s \in \mathbb{R}^{d_x \times d_x}$, dynamics map $g : \mathbb{R}^{d_x} \times \mathbb{R}^{d_x}$, measurement map $h : \mathbb{R}^{d_x} \times \mathbb{R}^{d_f} \times \mathbb{R}^{d_z}$, inverse measurement map $\ell : \mathbb{R}^{d_x} \times \mathbb{R}^{d_z} \times \mathbb{R}^{d_f}$, moving object dynamics map $g_o^\alpha : \mathbb{R}^{d_x} \times \mathbb{R}^{n_{of}(\alpha)d_f} \times \mathbb{R}^{n_{of}(\alpha)d_f}$ for each object indexed $\alpha \in [n_o]$, inverse moving object dynamics map $\gamma : \mathbb{R}^{n_{of}(\alpha)d_f} \times \mathbb{R}^{n_{of}(\alpha)d_f} \rightarrow \mathbb{R}^{d_x}$, time horizon $T \in \mathbb{N}$, number of features $n_f \in \mathbb{N}$, number of moving objects $n_o \in \mathbb{N}$.

Result: Estimates $\mu_t, \forall t \in \{0, 1, \dots, T\}$.

```

1  $\text{cost}_0 \leftarrow \|x_0 - \mu_0\|_{\Sigma_0^{-1}}^2$ 
2  $n_f, n_o \leftarrow 0$ .
3 for  $t = 0, 1, \dots, T-1$  do
4    $\{z_{t,k}^{(s)} : k \in [n_f + 1 : n_f + n'_f]\} \leftarrow$  Measurements of new static features.
5    $\mu_t, \Sigma_t, n_f \leftarrow$ 
6     Alg. 3, Dynamic EKF, (Static) Feature Augmentation
7   if  $n_o \geq 1$  then
8      $\{z_{t,\alpha,k}^{(m)} : \alpha \in [n_o], k \in [n_{of}(\alpha) + n_{of}(\alpha')]\} \leftarrow$ 
9       Measurements of  $n_{of}(\alpha)$  tracked and  $n_{of}(\alpha')$  new features of previously tracked moving objects indexed  $\alpha \in [n_o]$ .
10     $\mu_t, \Sigma_t \leftarrow$  Alg. 3, Dynamic EKF, (Dynamic) Feature Augmentation
11     $\mu_t, \Sigma_t \leftarrow$  Alg. 4, Dynamic EKF, (Dynamic) Object Pose Augmentation
12  end
13  if detect  $n'_o \geq 1$  new moving objects then
14     $\{z_{t,\alpha,k}^{(m)} : \alpha \in [n_o + 1 : n_o + n'_o], k \in [n_{of}(\alpha)]\} \leftarrow$ 
15      Measurements of features of new moving objects.
16     $\mu_t, \Sigma_t \leftarrow$  Alg. 3, Dynamic EKF, (Dynamic) Feature Augmentation
17     $n_o \leftarrow n_o + n'_o$ .
18  end
19   $\mu_t, \Sigma_t \leftarrow$  Alg. 6, Dynamic EKF, Smoothing Update
20   $\{z_{t,k}^{(s)} : k \in [n_f]\} \leftarrow$  Measurements of existing static features.
21   $\bar{\mu}_t, \bar{\Sigma}_t \leftarrow$  Alg. 5, Dynamic EKF, Static Feature Update
22   $\mu_{t+1}, \Sigma_{t+1} \leftarrow$  Alg. 7, Dynamic EKF, State Propagation
23 end
24 return  $\mu_0, \dots, \mu_T$ 

```

IV. DYNAMIC EKF-SLAM

Although the algorithms described in III can attain high estimation accuracy, their computation time often scales poorly with the number of moving objects or timesteps tracked. Inspired by the efficiency of filtering-based SLAM frameworks under the static world assumption, we use the unifying framework presented in Section II construct the dynamic EKF algorithm, described below, to address this issue.

At each time t , the dynamic EKF SLAM algorithm on Euclidean spaces maintains the full state vector:

$$\tilde{x}_t = (x_t, f^{(s)}, f^{(m)}, \xi) \in \mathbb{R}^{d_\mu}. \quad (4)$$

where $d_\mu := d_x + n_f d_f + 2 \cdot \sum_{\alpha=1}^{n_o} n_{of}(\alpha) d_f + (t-1) n_o d_x$. (For generality, we assume that all past moving object poses are maintained; in practice, these can be dropped). The components of \tilde{x}_t are as follows:

- **Ego robot pose:**

$x_t \in \mathbb{R}^{d_x}$ denotes the ego robot pose at the current time t .

- **Static feature position estimates:**

$f^{(s)} := (f_1^{(s)}, \dots, f_{n_f}^{(s)}) \in \mathbb{R}^{n_f d_f}$ is the position estimates of the $n_f \in \mathbb{N}$ static features currently tracked.

- **Moving object feature position estimates:**

$f^{(m)}$, defined below, is the feature positions of moving objects at the initial time 0 and the current time t . Here, $f_{\tau, \alpha, k}^{(m)} \in \mathbb{R}^{d_f}$ denotes the position estimate of the k -th feature of the moving object indexed α at time τ , for each $\tau \in \{0, t\}$, $\alpha \in [n_o]$, and $k \in [n_{of}(\alpha)]$, and $N_f := \sum_{\alpha=1}^{n_o} n_{of}(\alpha)$ denotes the total number of features summed over all moving objects:

$$\begin{aligned} f^{(m)} \\ := (f_{0,1,1}^{(m)}, \dots, f_{0,1,n_{of}(1)}^{(m)}, \dots, f_{0,n_o,1}^{(m)}, \dots, f_{0,1,n_{of}(n_o)}^{(m)}, \\ f_{t,1,1}^{(m)}, \dots, f_{t,1,n_{of}(1)}^{(m)}, \dots, f_{t,n_o,1}^{(m)}, \dots, f_{t,1,n_{of}(n_o)}^{(m)}) \\ \in \mathbb{R}^{2 \cdot N_f \cdot d_f}, \end{aligned}$$

For notational simplicity, we assume all features on all moving objects have been observed since the start of the time horizon. (This assumption can easily be relaxed).

- **Moving object poses:**

$\xi := (\xi_{1,1}, \dots, \xi_{1,n_o}, \dots, \xi_{t,1}, \dots, \xi_{t,n_o}) \in \mathbb{R}^{t n_o d_x}$ denotes the past and present poses of the n_o objects currently tracked. Here, $\xi_{\tau, \alpha} \in \mathbb{R}^{d_x}$ denotes the pose, of the moving object indexed $\alpha \in [n_o]$, at time τ , for each $\alpha \in [n_o]$ and $\tau \in [t]$. To ensure computational tractability, past pose estimates may be dropped.

Below, if unspecified, we assume the components in the full state $\tilde{x}_t \in \mathbb{R}$ appear in the order given in (4), i.e., $\tilde{x}_t = (x_t, f^{(s)}, f^{(m)}, \xi_t) \in \mathbb{R}^{d_\mu}$.

At initialization ($t = 0$), no feature or object has been detected ($n_f = n_o = 0$, $d_\mu = d_x$), and the dynamic EKF full state is simply the initial state $\tilde{x}_0 = x_0 \in \mathbb{R}^{d_x}$, with mean $\mu_0 \in \mathbb{R}^{d_x}$ and covariance $\Sigma_0 \in \mathbb{R}^{d_x \times d_x}$. Suppose, at the current time t , the running cost $c_{dEKF,t,0} : \mathbb{R}^{d_\mu} \rightarrow \mathbb{R}^{d_\mu}$ is:

$$c_{dEKF,t,0} = \|\tilde{x}_t - \mu_t\|_{\Sigma_t^{-1}}^2,$$

where $\tilde{x}_t \in \mathbb{R}^{d_\mu}$ denotes the EKF full state at time t , as described in the paragraphs above, with mean $\mu_t \in \mathbb{R}^{d_\mu}$ and symmetric positive definite covariance matrix $\Sigma_t \in \mathbb{R}^{d_\mu \times d_\mu}$.

Let $N_f := n_f + \sum_{\alpha=1}^{n_o} n_{of}(\alpha)$ denote the total number of features (static and moving) tracked at time t . First, the *feature augmentation step* appends position estimates of new features, denoted $f_{n_f+N_f+1}, \dots, f_{n_f+N_f+n'_f+N'_f} \in \mathbb{R}^{d_f}$ to the EKF full state \tilde{x}_t , and updates the mean and covariance of the full state. These new features may belong to static landmarks, previously detected moving objects, or new, previously undetected moving objects. Feature measurements $z_{t,n_f+N_f+1}, \dots, z_{t,n_f+N_f+n'_f+N'_f} \in \mathbb{R}^{d_z}$ are incorporated by adding measurement residual terms to the current running cost $c_{dEKF,t,0}$, resulting in a new cost $c_{dEKF,t,1} : \mathbb{R}^{d_\mu+(n'_f+N'_f)d_f} \rightarrow \mathbb{R}$:

$$c_{dEKF,t,1}(\tilde{x}_t, f_{t,n_f+N_f+1}, \dots, f_{t,n_f+N_f+N'_f})$$

$$:= \|\tilde{x}_t - \mu_t\|_{\Sigma_t^{-1}}^2 + \sum_{k=N_f+1}^{N_f+N'_f} \|z_{t,k} - h(x_t, f_{t,k})\|_{\Sigma_v^{-1}}^2.$$

In effect, $c_{dEKF,t,1}(\tilde{x}_t, f_{t,n_f+N_f+1}, \dots, f_{t,n_f+N_f+n'_f+N'_f})$ appends positions of new features to \tilde{x}_t , and constrains it using feature measurements residuals. A Gauss-Newton step then updates the mean $\mu_t \in \mathbb{R}^{d_\mu+N'_f d_f}$ and covariance $\Sigma_t \in \mathbb{R}^{(d_\mu+(n'_f+N'_f)d_f) \times (d_\mu+(n'_f+N'_f)d_f)}$ for \tilde{x}_t , resulting in a new cost:

$$c_{dEKF,t,2}(\tilde{x}_t) := \|\tilde{x}_t - \mu_t\|_{\Sigma_t^{-1}}^2.$$

We then increase d_μ by $N'_f d_f$, adjoin the new feature variables $(f_{t,n_f+N_f+1}, \dots, f_{t,n_f+N_f+n'_f+N'_f})$ to \tilde{x}_t , and rearrange the components of the full state \tilde{x}_t so that those new features associated with previously detected moving objects are stored alongside previously detected features for the same object (as determined by data association in the front end). If some new features correspond to a newly detected object, we store those features together as adjacent components in \tilde{x}_t , and accordingly increment n_o (the number of objects currently stored inside \tilde{x}_t). This restores the full state \tilde{x}_t to the form $(x_t, f^{(s)}, f^{(m)}, \xi_t) \in \mathbb{R}^{d_\mu}$ in (4).

The *moving object pose augmentation* step then appends pose estimates, denoted $\xi_{\alpha,t}$, for each tracked moving object $\alpha \in [n_o]$, relative to their initial pose. Moving objects' pose residual terms are added to the current running cost $c_{dEKF,t,2}$, resulting in a new cost $c_{dEKF,t,3} : \mathbb{R}^{d_\mu} \times \mathbb{R}^{n_o d_x} \rightarrow \mathbb{R}$:

$$\begin{aligned} c_{dEKF,t,3}(\tilde{x}_t, \xi_{t,1}, \dots, \xi_{t,n_o}) \\ = \|\tilde{x}_t - \mu_t\|_{\Sigma_t^{-1}}^2 + \|f_{t,\alpha}^{(m)} - g^o(\xi_{t,\alpha}, f_{t,\alpha}^{(m)})\|_{\Sigma_\xi^{-1}}^2. \end{aligned}$$

Essentially, $c_{dEKF,t,3}(\tilde{x}_t, \xi_{t,1}, \dots, \xi_{t,n_o})$ appends positions of new moving object poses to the full state \tilde{x}_t , and constrains it using the pose transform map $g^o : \mathbb{R}^{d_x} \times \mathbb{R}^{d_f} \rightarrow \mathbb{R}^{d_f}$. A Gauss-Newton step then constructs an updated mean $\mu_t \in \mathbb{R}^{d_\mu}$ and an updated covariance matrix $\Sigma_t \in \mathbb{R}^{d_\mu \times d_\mu}$ for \tilde{x}_t , resulting in a new cost $c_{dEKF,t,4}(\tilde{x}_t) : \mathbb{R}^{d_\mu+n_o d_x} \rightarrow \mathbb{R}$:

$$c_{dEKF,t,4}(\tilde{x}_t) := \|\tilde{x}_t - \mu_t\|_{\Sigma_t^{-1}}^2.$$

We adjoin the new moving object poses $(\xi_{t,1}, \dots, \xi_{t,n_o})$ to \tilde{x}_t (or record and drop them), then rearrange the components of the full state \tilde{x}_t so that each new moving object pose is stored alongside previously tracked poses for the same object. This restores the full state \tilde{x}_t to the form $(x_t, f^{(s)}, f^{(m)}, \xi_t) \in \mathbb{R}^{d_\mu}$, as introduced previously in (4).

Next, the *static feature update* step uses measurements of features contained in \tilde{x}_t to update the mean and covariance of \tilde{x}_t . More precisely, measurements $z_{t,1}^{(s)}, \dots, z_{t,n_f}^{(s)} \in \mathbb{R}^{d_z}$, of the n_f static features $f_1^{(s)}, \dots, f_{n_f}^{(s)} \in \mathbb{R}^{d_f}$ currently tracked in \tilde{x}_t , are introduced by incorporating associated measurement residuals to the running cost, resulting in a new cost $c_{dEKF,t,5} : \mathbb{R}^{d_\mu} \rightarrow \mathbb{R}$:

$$\begin{aligned} c_{dEKF,t,5}(\tilde{x}_t) \\ := \|\tilde{x}_t - \mu_t\|_{\Sigma_t^{-1}}^2 + \sum_{k=1}^{n_f} \|z_{t,k} - h(x_t, f_{t,k}^{(s)})\|_{\Sigma_v^{-1}}^2. \end{aligned}$$

A Gauss-Newton step then constructs an updated mean $\mu_t \in \mathbb{R}^{d_\mu}$ and covariance $\Sigma_t \in \mathbb{R}^{d_\mu \times d_\mu}$ for \tilde{x}_t , resulting in a new cost $c_{dEKF,t,6} : \mathbb{R}^{d_\mu} \rightarrow \mathbb{R}$:

$$c_{dEKF,t,6}(\tilde{x}_t) := \|\tilde{x}_t - \mu_t\|_{\Sigma_t^{-1}}^2,$$

of the form of $c_{dEKF,t,0}$.

The *smoothing update* step then updates the three most recent tracked dynamic object poses, denoted $\{\xi_{\tau,\alpha} : \tau \in \{t-2, t-1, t\}, \alpha \in [n_o]\}$, by ensuring that the object's motion from time $t-2$ to time $t-1$ does not deviate significantly from its motion from time $t-1$ to time t . This regularization process ensures that the estimated trajectories of the moving objects are smooth enough to be physically feasible. To this end, we define a new cost $c_{dEKF,t,7} : \mathbb{R}^{d_\mu} \rightarrow \mathbb{R}$:

$$\begin{aligned} c_{dEKF,t,7}(\tilde{x}_t) \\ := \|\tilde{x}_t - \mu_t\|_{\Sigma_t^{-1}}^2 + \sum_{\alpha=1}^{n_o} \|\mathbf{s}(\xi_{t-2,\alpha}, \xi_{t-1,\alpha}, \xi_{t,\alpha})\|_{\Sigma_s^{-1}}^2. \end{aligned}$$

We then apply a Gauss-Newton step to update the mean $\mu_t \in \mathbb{R}^{d_\mu}$ and covariance $\Sigma_t \in \mathbb{R}^{d_\mu \times d_\mu}$, resulting in a new cost:

$$c_{dEKF,t,8}(\tilde{x}_t) := \|\tilde{x}_t - \mu_t\|_{\Sigma_t^{-1}}^2.$$

that has the form of the original cost $c_{dEKF,t,0}$.

Finally, the *state propagation* step propagates the EKF full state forward by one time step, via the EKF state propagation map $g : \mathbb{R}^{d_\mu} \rightarrow \mathbb{R}^{d_\mu}$. To propagate \tilde{x}_t forward in time, we incorporate the dynamics residual to the running cost, resulting in a new cost $c_{dEKF,t,9} : \mathbb{R}^{d_\mu} \rightarrow \mathbb{R}$:

$$\begin{aligned} c_{dEKF,t,9}(\tilde{x}_t, x_{t+1}) \\ := \|\tilde{x}_t - \mu_t\|_{\Sigma_t^{-1}}^2 + \|x_{t+1} - g(x_t)\|_{\Sigma_w^{-1}}^2. \end{aligned}$$

In effect, $c_{dEKF,t,9}$ appends the new state $x_{t+1} \in \mathbb{R}^{d_x}$ to \tilde{x}_t , while adding a new cost posed by the dynamics residuals. A marginalization step, with $\tilde{x}_{t,K} := (x_{t+1}, f^{(s)}, f^{(m)}, \xi) \in \mathbb{R}^{d_\mu}$ and $\tilde{x}_{t,M} := x_t \in \mathbb{R}^{d_x}$, then removes the previous state $x_t \in \mathbb{R}^{d_x}$ from the running cost. This step produces a mean $\mu_{t+1} \in \mathbb{R}^{d_\mu}$ and a covariance $\Sigma_{t+1} \in \mathbb{R}^{d_\mu \times d_\mu}$ for the new EKF full state, $\tilde{x}_{t+1} := \tilde{x}_{t,K} = (x_{t+1}, f^{(s)}, f^{(m)}, \xi)$. The running cost is updated to $c_{dEKF,t+1,0} : \mathbb{R}^{d_\mu} \rightarrow \mathbb{R}$:

$$c_{dEKF,t+1,0}(\tilde{x}_{t+1}) := \|\tilde{x}_{t+1} - \mu_{t+1}\|_{\Sigma_{t+1}^{-1}}^2,$$

of the form of $c_{dEKF,t,0}$.

The theorems below establish the mathematical equivalence of the five steps of the dynamic EKF, as presented above in our optimization framework (Alg. 1), to those presented in the extension standard EKF SLAM algorithm to a dynamic setting (Alg. 2). Theorem statements and proofs concerning the equivalence of the feature augmentation, feature update, and state propagation steps are identical to those in the static EKF-SLAM case, and are omitted for brevity. For more details, please see Appendix A, or [1], Theorems 5.1-5.3.

Theorem 4.1: The dynamic object pose augmentation step of standard-formulation dynamic EKF SLAM (Alg. 4) is equivalent to applying a Gauss-Newton step to $c_{dEKF,t,3} : \mathbb{R}^{d_\mu+n_o d_x} \rightarrow \mathbb{R}$, with:

$$c_{dEKF,t,3}(\tilde{x}_t, \xi_{t,1}, \dots, \xi_{t,n_o})$$

$$:= \|\tilde{x}_t - \mu_t\|_{\Sigma_t^{-1}}^2 + \sum_{\alpha=1}^{n_o} \sum_{k=1}^{n_{of}(\alpha)} \|f_{t,\alpha,k}^{(m)} - g^o(\xi_{t,\alpha}, f_{0,\alpha,k}^{(m)})\|_{\Sigma_\xi^{-1}}^2.$$

when Σ_ξ is a diagonal matrix. ■

Proof: See Appendix A. ■

Theorem 4.2: The smoothing update step of standard-formulation dynamic EKF SLAM (Alg. 6) is equivalent to applying a Gauss-Newton step to $c_{dEKF,t,7} : \mathbb{R}^{d_\mu} \rightarrow \mathbb{R}$, with:

$$\begin{aligned} c_{dEKF,t,7}(\tilde{x}_t) \\ := \|\tilde{x}_t - \mu_t\|_{\Sigma_t^{-1}}^2 + \sum_{\alpha=1}^{n_o} \|\mathbf{s}(\xi_{t-2,\alpha}, \xi_{t-1,\alpha}, \xi_{t,\alpha})\|_{\Sigma_s^{-1}}^2. \end{aligned}$$

Proof: See Appendix A. ■

V. EXPERIMENTS

To illustrate the estimation accuracy and mapping precision of the dynamic EKF algorithm presented above, we constructed a simulated driving scenario (Figure 1). In the scenario, the ego vehicle navigates alongside two other vehicles (Agents 1, 2) and a pedestrian (Agent 3) on a highway with three lanes, while simultaneously tracking the positions of non-ego vehicles and fixed landmarks in its surroundings. As time progresses, the vehicles change lanes and adjust their velocities. Object motion is sampled every 0.5 s for 60 s to form a ground truth dataset.

To test our dynamic EKF algorithm, we performed Monte Carlo experiments on the simulated driving setting described above. For each combination of the three odometry and image measurement noise covariance levels given below, we simulated the ground truth trajectory 25 times, each with independently generated errors:

$$\Sigma_{w,1} := \begin{bmatrix} 10^{-6} & 0 & 0 \\ 0 & 10^{-6} & 0 \\ 0 & 0 & 10^{-8} \end{bmatrix}, \Sigma_{v,1} := 10^{-6} \cdot I_{2 \times 2}, \quad (5)$$

$$\Sigma_{w,2} := \begin{bmatrix} 10^{-5} & 0 & 0 \\ 0 & 10^{-5} & 0 \\ 0 & 0 & 10^{-7} \end{bmatrix}, \Sigma_{v,2} := 10^{-5} \cdot I_{2 \times 2}, \quad (6)$$

$$\Sigma_{w,3} := \begin{bmatrix} 10^{-4} & 0 & 0 \\ 0 & 10^{-4} & 0 \\ 0 & 0 & 10^{-6} \end{bmatrix}, \Sigma_{v,3} := 10^{-4} \cdot I_{2 \times 2}, \quad (7)$$

Here, $I_{2 \times 2}$ denotes the 2×2 identity matrix, and each entry of the above matrices has unit m^2 (meters squared). We then applied dynamic EKF SLAM to recover the ground truth trajectory, and computed the resulting root-mean-squared error for each noise level (Table I). By dropping past poses of all moving objects, each simulation can be run on a standard, single-threaded laptop in under 37 ms. We observed that our estimation accuracy decreased gracefully as the noise level increased. For more details regarding the simulation setup and results, please see Appendix C.

VI. CONCLUSION AND FUTURE WORK

In this tutorial, we extended the unifying optimization-based SLAM backend framework in [1] to environments with moving objects. We use this framework to describe the

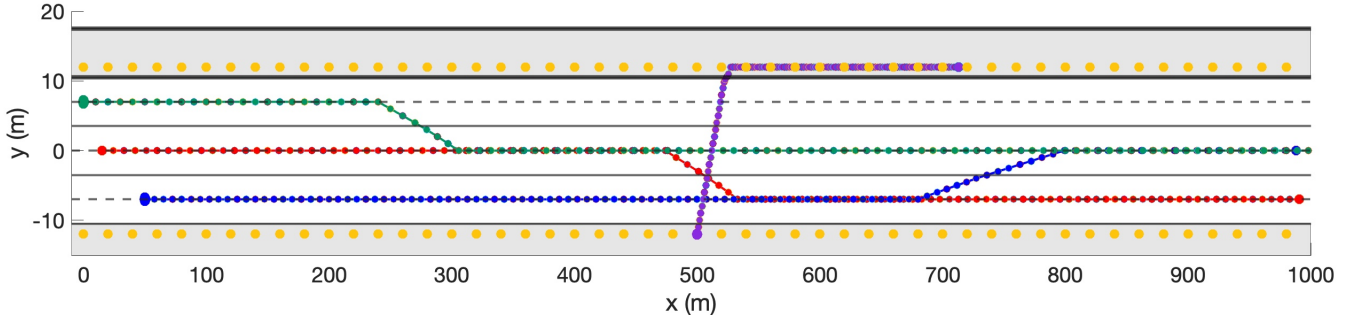


Fig. 1. Schematic for the ground truth trajectory of the driving example. The ego vehicle (red) navigates and runs dynamic EKF SLAM along a kilometer-long stretch of highway, from left to right, alongside two other vehicles (green, blue) and a jaywalking pedestrian (purple). Static landmarks (yellow) are scattered throughout the scene. Initial feature estimates of each moving object are plotted, but are not clearly visible due to the schematic scale.

Noise Level	Data	Ego Poses	Static Features	Agent 1 Features	Agent 2 Features	Agent 3 Features	Agent 1 Poses	Agent 2 Poses	Agent 3 Poses
$\Sigma_{w,1}, \Sigma_{v,1}$	x (m)	0.008	0.014	0.014	0.014	0.014	0.001	0.001	0.001
	y (m)	0.032	0.028	0.003	0.001	0.025	0.028	0.035	0.006
	θ (rad)	0.000	N/A	N/A	N/A	N/A	0.001	0.001	0.006
$\Sigma_{w,1}, \Sigma_{v,2}$	x (m)	0.035	0.062	0.062	0.062	0.063	0.002	0.002	0.002
	y (m)	0.061	0.059	0.007	0.003	0.052	0.054	0.066	0.012
	θ (rad)	0.000	N/A	N/A	N/A	N/A	0.004	0.004	0.015
$\Sigma_{w,1}, \Sigma_{v,3}$	x (m)	0.089	0.155	0.157	0.157	0.156	0.005	0.004	0.006
	y (m)	0.152	0.157	0.168	0.009	0.138	0.137	0.166	0.032
	θ (rad)	0.000	N/A	N/A	N/A	N/A	0.011	0.011	0.054
$\Sigma_{w,2}, \Sigma_{v,1}$	x (m)	0.008	0.012	0.012	0.012	0.012	0.002	0.002	0.003
	y (m)	0.072	0.053	0.004	0.004	0.046	0.065	0.080	0.014
	θ (rad)	0.000	N/A	N/A	N/A	N/A	0.001	0.001	0.005
$\Sigma_{w,2}, \Sigma_{v,2}$	x (m)	0.028	0.048	0.049	0.048	0.050	0.003	0.003	0.004
	y (m)	0.088	0.0074	0.007	0.005	0.065	0.078	0.004	0.018
	θ (rad)	0.000	N/A	N/A	N/A	N/A	0.004	0.004	0.016
$\Sigma_{w,2}, \Sigma_{v,3}$	x (m)	0.103	0.181	0.182	0.182	0.182	0.005	0.005	0.007
	y (m)	0.200	0.196	0.020	0.010	0.173	0.180	0.217	0.041
	θ (rad)	0.000	N/A	N/A	N/A	N/A	0.012	0.012	0.053
$\Sigma_{w,3}, \Sigma_{v,1}$	x (m)	0.017	0.017	0.019	0.016	0.021	0.009	0.008	0.012
	y (m)	0.287	0.232	0.016	0.012	0.202	0.259	0.317	0.058
	θ (rad)	0.001	N/A	N/A	N/A	N/A	0.001	0.001	0.005
$\Sigma_{w,3}, \Sigma_{v,2}$	x (m)	0.029	0.043	0.044	0.044	0.045	0.010	0.009	0.013
	y (m)	0.226	0.164	0.015	0.009	0.144	0.200	0.246	0.044
	θ (rad)	0.001	N/A	N/A	N/A	N/A	0.004	0.004	0.016
$\Sigma_{w,3}, \Sigma_{v,3}$	x (m)	0.093	0.161	0.161	0.010	0.014	0.010	0.010	0.014
	y (m)	0.312	0.264	0.027	0.014	0.233	0.277	0.340	0.061
	θ (rad)	0.001	N/A	N/A	N/A	N/A	0.012	0.013	0.053

TABLE I

ROOT-MEAN-SQUARED TRANSLATION (x, y) AND ROTATION (θ) ERROR ON OUR SIMULATED DRIVING DATASET. NOISE LEVEL SETTINGS CORRESPOND TO DIFFERENT CHOICES OF Σ_w AND Σ_v (WITH $\Sigma_0 = \Sigma_w$), AS DEFINED IN 5, 6, 7. ROOT-MEAN-SQUARED ERRORS ARE AVERAGED OVER 25 EXPERIMENTS FOR EACH NOISE SETTING.

back-ends of recently proposed dynamic SLAM algorithms [5, 6, 8, 9]. To establish a rapprochement with filtering-based SLAM methods, we apply a aggressive marginalization scheme in our framework to derive the dynamic EKF SLAM algorithm, which we prove to be mathematically identical to the straightforward extension of the conventional EKF-SLAM algorithm to environments with moving objects. Simulation results indicate that dynamic EKF-SLAM performs well in pose estimation, as well as static and dynamic feature tracking.

The formulation presented in this tutorial can be refined in several ways. First, we are eager to deploy our framework on real-world data, and explore the tradeoffs inherent in different design choices. Second, many robotics applications require topological and/or semantic maps of dynamic scenes,

in addition to purely metric information. Thus, dynamic object features should be explicitly encoded in our framework as lower-dimensional semantic representations, e.g., bounding boxes, as is done in existing methods [5, 8, 9]. Third, robust formulations of our framework must allow for the implementation of multi-hypothesis SLAM backends, to reliably safeguard against ambiguous data associations or high outlier densities. [13, 14]. Finally, guidelines for selecting appropriate modeling choices within our dynamic SLAM framework depend heavily on downstream tasks, such as autonomous navigation in the presence of multiple agents [15, 16]. It is of interest to design complete autonomy stacks that fully harness the flexibility of our dynamic SLAM framework for estimation, prediction, and planning in challenging robotics tasks.

Algorithm 3: Dynamic EKF, Feature Augmentation Sub-block.

Data: Current EKF state $\tilde{x}_t \in \mathbb{R}^{d_\mu}$, with mean μ_t , and covariance Σ_t ; number of static features $n_f \in \mathbb{N}$; total number of features on moving objects $N_f \in \mathbb{N}$; measurements of new features $z_{t,k} \in \mathbb{R}^{d_z}$, $k \in [n_f + N_f + 1 : n_f + N_f + n'_f + N'_f]$; measurement map $h : \mathbb{R}^{d_x} \times \mathbb{R}^{d_f} \rightarrow \mathbb{R}^{d_z}$; inverse measurement map $\ell : \mathbb{R}^{d_x} \times \mathbb{R}^{d_z} \rightarrow \mathbb{R}^{d_f}$, with $z_{t,k} = h(x_t, \ell(x_t, z_{t,k})) \forall x_t \in \mathbb{R}^{d_x}$.

Result: Updated number of static features n_f ; updated total number of features on moving objects N_f , updated EKF state dimension d_μ , updated EKF state mean $\mu_t \in \mathbb{R}^{d_\mu}$, covariance $\Sigma_t \in \mathbb{R}^{d_\mu \times d_\mu}$

- 1 $(\mu_{t,x}, \mu_{t,e}) \leftarrow \mu_t$, with $\mu_{t,x} \in \mathbb{R}^{d_x}$.
- 2 $\ell(\mu_{t,x}, z_{t,n_f+N_f+1}, \dots, z_{t,n_f+N_f+n'_f+N'_f}) \leftarrow (\ell(\mu_{t,x}, z_{t,n_f+N_f+1}), \dots, \ell(\mu_{t,x}, z_{t,n_f+N_f+n'_f+N'_f})) \in \mathbb{R}^{(n'_f+N'_f)d_f}$, with $\ell : \mathbb{R}^{d_x+N'_f d_z} \rightarrow \mathbb{R}^{N'_f d_f}$
- 3 $\mu_t \leftarrow (\mu_t, \ell(\mu_{t,x}, z_{t,n'_f+N'_f+1}, \dots, z_{t,n_f+N_f+n'_f+N'_f})) \in \mathbb{R}^{d_\mu+(n'_f+N'_f)d_f}$
- 4 $\begin{bmatrix} \Sigma_{t,xx} & \Sigma_{t,xe} \\ \Sigma_{t,ex} & \Sigma_{t,ee} \end{bmatrix} \leftarrow \Sigma_t$, with $\Sigma_{t,xx} \in \mathbb{R}^{d_x \times d_x}$
- 5 $L_x \leftarrow \frac{\partial \ell}{\partial x} \Big|_{\mu_t} \in \mathbb{R}^{(n'_f+N'_f)d_f \times d_x}$
- 6 $L_z \leftarrow \frac{\partial \ell}{\partial z} \Big|_{\mu_t} \in \mathbb{R}^{(n'_f+N'_f)d_f \times (n'_f+N'_f)d_z}$
- 7 $\tilde{\Sigma}_v \leftarrow \text{diag}\{\Sigma_v, \dots, \Sigma_v\} \in \mathbb{R}^{(n'_f+N'_f)d_z \times (n'_f+N'_f)d_z}$
- 8 $\Sigma_t \leftarrow \begin{bmatrix} \Sigma_{t,xx} & \Sigma_{t,xe} & \Sigma_{t,xx} L_x^\top \\ \Sigma_{t,ex} & \Sigma_{t,ee} & \Sigma_{t,ex} L_x^\top \\ L_x \Sigma_{t,xx} & L_x \Sigma_{t,xe} & L_x \Sigma_{t,xx} L_x^\top + L_z \tilde{\Sigma}_v L_z^\top \end{bmatrix} \in \mathbb{R}^{(d_\mu+(n'_f+N'_f)d_f) \times (d_\mu+(n'_f+N'_f)d_f)}$
- 9 $\tilde{x}_t \leftarrow (\tilde{x}_t, f_{t,N_f+1}, \dots, f_{t,N_f+N'_f}) \in \mathbb{R}^{d_\mu+(n'_f+N'_f)d_f}$
- 10 $n_f \leftarrow n_f + n'_f$
- 11 $N_f \leftarrow N_f + N'_f$
- 12 $d_\mu \leftarrow d_\mu + (n'_f + N'_f)d_f$
- 13 Reorder variables in \tilde{x}_t to restore the variable ordering of (4).
- 14 **return** $N_f, d_\mu, \mu_t, \Sigma_t$.

REFERENCES

- [1] Amay Saxena, Chih-Yuan Chiu, Ritika Shrivastava, Joseph Menke, and Shankar Sastry. “Simultaneous Localization and Mapping: Through the Lens of Nonlinear Optimization”. In: *IEEE Robotics and Automation Letters* 7.3 (2022), pp. 7148–7155. DOI: 10.1109/LRA.2022.3181409.
- [2] J.J. Leonard and H.F. Durrant-Whyte. “Simultaneous Map Building and Localization for an Autonomous Mobile Robot”. In: *IEEE IROS*. Vol. 3. 1991, pp. 1442–7.
- [3] C. Cadena, L. Carlone, H. Carrillo, Y. Latif, D. Scaramuzza, J. Neira, I. Reid, and J. J. Leonard. “Past, Present, and Future of Simultaneous Localization and Mapping: Toward the Robust-Perception Age”. In: *IEEE T-RO* 32.6 (2016), pp. 1309–1332.
- [4] Chieh-Chih Wang, Charles Thorpe, Sebastian Thrun, Martial Hebert, and Hugh Durrant-Whyte. “Simultaneous Localization, Mapping and Moving Object Tracking”. In: *The International Journal of Robotics Research* 26.9 (2007), pp. 889–916. DOI: 10.1177/0278364907081229. eprint: <https://doi.org/10.1177/0278364907081229>. URL: <https://doi.org/10.1177/0278364907081229>.
- [5] Shichao Yang and Sebastian Scherer. “CubeSLAM: Monocular 3-D Object SLAM”. In: *IEEE Transactions on Robotics* 35.4 (2019), pp. 925–938. DOI: 10.1109/TRO.2019.2909168.
- [6] Jiahui Huang, Sheng Yang, Zishuo Zhao, Yu-Kun Lai, and Shi-Min Hu. “ClusterSLAM: A SLAM Backend for Simultaneous Rigid Body Clustering and Motion Estimation”. In: *Proceed-*

Algorithm 4: Dynamic EKF, Moving Object Pose Augmentation Sub-block.

Data: Current EKF state $\tilde{x}_t \in \mathbb{R}^{d_\mu}$ mean μ_t and covariance Σ_t ; number of dynamic objects n_o with features detected at times 0 and t ; inverse moving object dynamics map $\gamma^\alpha : \mathbb{R}^{d_x} \times \mathbb{R}^{d_x} \rightarrow \mathbb{R}^{d_x}$, satisfying $\xi = \gamma(f, g^o(\xi, f))$ for each $f, f' \in \mathbb{R}^{n_{of}(\alpha)d_f}$; moving object dynamics noise covariance $\tilde{\Sigma}_\xi \in \mathbb{R}^{d_x \times d_x}$; number of features $n_{of}(\alpha) \in \mathbb{N}$ detected on each moving object with index $\alpha \in [n_o]$.

Result: Updated EKF state dimension d_μ , updated EKF state mean $\mu_t \in \mathbb{R}^{d_\mu}$, covariance $\Sigma_t \in \mathbb{R}^{d_\mu \times d_\mu}$.

- 1 $N_f \leftarrow \sum_{\alpha=1}^{n_o} n_{of}(\alpha)$
- 2 $f_{\tau,\alpha}^{(m)} \leftarrow (f_{\tau,\alpha,1}^{(m)}, \dots, f_{\tau,\alpha,n_{of}(\alpha)}^{(m)}) \in \mathbb{R}^{n_{of}(\alpha) \cdot d_f}$, $\forall \alpha \in [n_o], \tau \in \{0, t\}$
- 3 $f_\tau^{(m)} \leftarrow (f_{\tau,1}^{(m)}, \dots, f_{\tau,n_o}^{(m)}) \in \mathbb{R}^{N_f d_f}$, $\forall \tau \in \{0, t\}$
- 4 $\xi_t \leftarrow (\xi_{t,1}, \dots, \xi_{t,n_o}) \in \mathbb{R}^{n_o d_x}$.
- 5 Reorder variables in \tilde{x}_t so that $f_0^{(m)}, f_t^{(m)}$ appear last.
- 6 $\begin{bmatrix} \Sigma_{t,ee} & \Sigma_{t,ef} & \Sigma_{t,ef'} \\ \Sigma_{t,fe} & \Sigma_{t,ff} & \Sigma_{t,ff'} \\ \Sigma_{t,f'e} & \Sigma_{t,f'f} & \Sigma_{t,f'f'} \end{bmatrix} \leftarrow \Sigma_t$, with $\Sigma_{t,ff}, \Sigma_{t,f'f'} \in \mathbb{R}^{N_f d_f \times N_f d_f}$
- 7 $\tilde{\gamma}(f_0^{(m)}, f_t^{(m)}) \leftarrow (\gamma(f_{0,1}^{(m)}, f_{t,1}^{(m)}), \dots, \gamma(f_{0,n_o}^{(m)}, f_{t,n_o}^{(m)})) \in \mathbb{R}^{n_o d_x}$, with $\tilde{\gamma} : \mathbb{R}^{N_f d_f} \times \mathbb{R}^{N_f d_f} \rightarrow \mathbb{R}^{n_o d_x}$
- 8 $\tilde{g}^o(\xi_t, f_0^{(m)}) \leftarrow (g^o(\xi_{t,1}, f_{0,1}^{(m)}), \dots, \xi_{t,n_o}, f_{0,n_o}^{(m)})) \in \mathbb{R}^{N_f d_f}$
- 9 $\tilde{G}_\xi \leftarrow \frac{\partial \tilde{g}^o}{\partial \xi}(\xi_t, f_0^{(m)})$
- 10 $\tilde{\Gamma}_1 \leftarrow \frac{\partial \tilde{\gamma}}{\partial f_{0,n_o}^{(m)}} \Big|_{f_{0,n_o}^{(m)}} \in \mathbb{R}^{n_o d_x \times (d_\mu - 2N_f d_f)}$
- 11 $\tilde{\Gamma}_2 \leftarrow \frac{\partial \tilde{\gamma}}{\partial f_{t,n_o}^{(m)}} \Big|_{f_{t,n_o}^{(m)}} \in \mathbb{R}^{n_o d_x \times N_f d_f}$
- 12 $\mu_t \leftarrow (\mu_t, \tilde{\gamma}(f_0^{(m)}, f_t^{(m)})) \in \mathbb{R}^{d_\mu + n_o d_x}$
- 13 $\Sigma_{t,ee} \leftarrow \tilde{\Gamma}_1 \Sigma_{t,fe} + \tilde{\Gamma}_2 \Sigma_{t,f'e} \in \mathbb{R}^{n_o d_x \times (d_\mu - 2N_f d_f)}$
- 14 $\Sigma_{t,ef} \leftarrow \tilde{\Gamma}_1 \Sigma_{t,ff} + \tilde{\Gamma}_2 \Sigma_{t,f'f} \in \mathbb{R}^{n_o d_x \times N_f d_f}$
- 15 $\Sigma_{t,f'e} \leftarrow \tilde{\Gamma}_1 \Sigma_{t,ff'} + \tilde{\Gamma}_2 \Sigma_{t,f'f'} \in \mathbb{R}^{n_o d_x \times N_f d_f}$
- 16 $\Sigma_{t,ef'} \leftarrow \tilde{\Gamma}_1 \Sigma_{t,ff} \tilde{\Gamma}_1^\top + \tilde{\Gamma}_2 \Sigma_{t,f'f} \tilde{\Gamma}_1^\top + \tilde{\Gamma}_1 \Sigma_{t,ff'} \tilde{\Gamma}_2^\top + \tilde{\Gamma}_2 \Sigma_{t,f'f'} \tilde{\Gamma}_2^\top \in \mathbb{R}^{n_o d_x \times n_o d_x}$
- 17 $\Sigma_t \leftarrow \begin{bmatrix} \Sigma_{t,ee} & \Sigma_{t,ef} & \Sigma_{t,ef'} & \Sigma_{t,ef}^\top \xi_e \\ \Sigma_{t,fe} & \Sigma_{t,ff} & \Sigma_{t,ff'} & \Sigma_{t,fe}^\top \xi_f \\ \Sigma_{t,f'e} & \Sigma_{t,f'f} & \Sigma_{t,f'f'} & \Sigma_{t,f'e}^\top \xi_{f'} \\ \Sigma_{t,ef}^\top \xi_e & \Sigma_{t,ff}^\top \xi_f & \Sigma_{t,ff'}^\top \xi_{f'} & \Sigma_{t,ef}^\top \xi_{f'} \end{bmatrix} \in \mathbb{R}^{(d_\mu + n_o d_x) \times (d_\mu + n_o d_x)}$
- 18 $d_\mu \leftarrow d_\mu + n_o d_x$
- 19 Reorder variables in \tilde{x}_t to restore the variable ordering of (4).
- 20 **return** d_μ, μ_t, Σ_t .

ings of the IEEE/CVF International Conference on Computer Vision (ICCV). Oct. 2019.

- [7] Berta Bescos, José M. Fácil, Javier Civera, and José Neira. “DynaSLAM: Tracking, Mapping and Inpainting in Dynamic Scenes”. In: 2018.
- [8] Berta Bescos, Carlos Campos, Juan D. Tardós, and José Neira. “DynaSLAM II: Tightly-Coupled Multi-Object Tracking and SLAM”. In: *IEEE Robotics and Automation Letters* 6 (2021), pp. 5191–5198.
- [9] J. Zhang, M. Heneini, R. Mahony, and V. Ila. “VDO-SLAM: A Visual Dynamic Object-aware SLAM System”. In: *arXiv*. 2020. arXiv: 2005.11052 [cs.RO].
- [10] S. Thrun, W. Burgard, and D. Fox. *Probabilistic Robotics*. The MIT Press, 2005.
- [11] Raúl Mur-Artal and Juan D. Tardós. “ORB-SLAM2: An Open-Source SLAM System for Monocular, Stereo, and RGB-D Cameras”. In: *IEEE Transactions on Robotics* 33.5 (2017), pp. 1255–1262. DOI: 10.1109/TRO.2017.2705103.

Algorithm 5: Dynamic EKF, Static Feature Update Sub-block.

Data: Prior $\mathcal{N}(\mu_0, \Sigma_0)$ on $x_0 \in \mathbb{R}^{d_x}$, noise covariances $\Sigma_w \in \mathbb{R}^{d_x \times d_x}$, $\Sigma_v \in \mathbb{R}^{d_z \times d_z}$, $\Sigma_\xi \in \mathbb{R}^{d_x \times d_x}$, $\Sigma_s \in \mathbb{R}^{d_x \times d_x}$, dynamics map $g: \mathbb{R}^{d_x} \times \mathbb{R}^{d_x}$, measurement map $h: \mathbb{R}^{d_x} \times \mathbb{R}^{d_f} \times \mathbb{R}^{d_z}$, inverse measurement map $\tilde{h}: \mathbb{R}^{d_x} \times \mathbb{R}^{d_z} \times \mathbb{R}^{d_f}$, moving object dynamics map $g_o^\alpha: \mathbb{R}^{d_x} \times \mathbb{R}^{n_{of}(\alpha)d_f} \times \mathbb{R}^{n_{of}(\alpha)d_f}$ for each object indexed $\alpha \in [n_o]$; time horizon $T \in \mathbb{N}$; number of features $n_f \in \mathbb{N}$; number of moving objects $n_o \in \mathbb{N}$.

Result: Updated EKF state mean $\mu_t \in \mathbb{R}^{d_\mu}$, covariance $\Sigma_t \in \mathbb{R}^{d_\mu \times d_\mu}$

- 1 $f^{(s)} \leftarrow (f_1^{(s)}, \dots, f_{n_f}^{(s)}) \in \mathbb{R}^{n_f d_f}$
- 2 $\tilde{h}(x_t, f^{(s)}) \leftarrow (h(x_t, f_1^{(s)}), \dots, h(x_t, f_{n_f}^{(s)})) \in \mathbb{R}^{n_f d_z}$
- 3 $H_t \leftarrow \frac{\partial \tilde{h}}{\partial (x_t, f^{(s)})} \Big|_{\mu_t} \in \mathbb{R}^{n_f d_z \times (d_x + n_f d_f)}$
- 4 $\tilde{\Sigma}_v \leftarrow \text{diag}\{\Sigma_v, \dots, \Sigma_v\} \in \mathbb{R}^{n_f d_z \times n_f d_z}$
- 5 $\bar{\mu}_t \leftarrow$

$$\mu_t + \Sigma_t \begin{bmatrix} H_t^\top \\ O \end{bmatrix} \left([H_t \ O] \Sigma_t \begin{bmatrix} H_t^\top \\ O \end{bmatrix} + \tilde{\Sigma}_v \right)^{-1} (z_{t,1:n_f} - \tilde{h}(\mu_t, f^{(s)})) \in \mathbb{R}^{d_\mu}$$
- 6 $\bar{\Sigma}_t \leftarrow \Sigma_t -$

$$\Sigma_t \begin{bmatrix} H_t^\top \\ O \end{bmatrix} \left([H_t \ O] \Sigma_t \begin{bmatrix} H_t^\top \\ O \end{bmatrix} + \tilde{\Sigma}_v \right)^{-1} [H_t \ O] \Sigma_t \in \mathbb{R}^{d_\mu \times d_\mu}$$
- 7 **return** μ_t, Σ_t .

Algorithm 6: Dynamic EKF, Smoothing Update Sub-block.

Data: Current EKF state $\tilde{x}_t \in \mathbb{R}^{d_\mu}$, with mean μ_t and covariance Σ_t , smoothing covariance $\Sigma_s \in \mathbb{R}^{d_x \times d_x}$, number of dynamic objects $\alpha \in [n_o]$ with poses $\xi_{\tau,\alpha}$ tracked at times $\tau \in \{t-2, t-1, t\}$.

Result: Updated EKF state mean $\mu_t \in \mathbb{R}^{d_\mu}$, covariance $\Sigma_t \in \mathbb{R}^{d_\mu \times d_\mu}$.

- 1 $\xi_\tau \leftarrow (\xi_{\tau,1}, \dots, \xi_{\tau,n_o}) \in \mathbb{R}^{n_o d_x}, \forall \tau \in \{t-2, t-1, t\}$
- 2 Reorder variables in \tilde{x}_t such that $(\xi_{t-2}, \xi_{t-1}, \xi_t) \in \mathbb{R}^{3n_o d_x}$ appears last.
- 3 $\tilde{\Sigma}_s \leftarrow \text{diag}\{\Sigma_s, \dots, \Sigma_s\} \in \mathbb{R}^{n_o d_x \times n_o d_x}$
- 4 $\tilde{s}(\xi_{t-2}, \xi_{t-1}, \xi_t) \leftarrow$

$$(s(\xi_{t-2,1}, \xi_{t-1,1}, \xi_{t,1}), \dots, s(\xi_{t-2,n_o}, \xi_{t-1,n_o}, \xi_{t,n_o})) \in \mathbb{R}^{n_o d_x}$$
- 5 $\tilde{S}_\tau \leftarrow \frac{\partial \tilde{s}}{\partial \xi_\tau}, \text{ for each } \tau \in \{t-2, t-1, t\}$.
- 6 $\mu_t \leftarrow \mu_t -$

$$\Sigma_t \begin{bmatrix} O \\ \tilde{S}_{t-2}^\top \\ \tilde{S}_{t-1}^\top \\ \tilde{S}_t^\top \end{bmatrix} \left(\tilde{\Sigma}_s + [O \ \tilde{S}_{t-2} \ \tilde{S}_{t-1} \ \tilde{S}_t] \Sigma_t^{-1} \begin{bmatrix} O \\ \tilde{S}_{t-2}^\top \\ \tilde{S}_{t-1}^\top \\ \tilde{S}_t^\top \end{bmatrix} \right)^{-1}$$

$$s(\xi_{t-2}, \xi_{t-1}, \xi_t) \in \mathbb{R}^{d_\mu}$$
- 7 $\Sigma_t \leftarrow \Sigma_t -$

$$\Sigma_t \begin{bmatrix} O \\ \tilde{S}_{t-2}^\top \\ \tilde{S}_{t-1}^\top \\ \tilde{S}_t^\top \end{bmatrix} \left(\tilde{\Sigma}_s + [O \ \tilde{S}_{t-2} \ \tilde{S}_{t-1} \ \tilde{S}_t] \Sigma_t^{-1} \begin{bmatrix} O \\ \tilde{S}_{t-2}^\top \\ \tilde{S}_{t-1}^\top \\ \tilde{S}_t^\top \end{bmatrix} \right)^{-1}$$

$$\cdot [O \ \tilde{S}_{t-2} \ \tilde{S}_{t-1} \ \tilde{S}_t] \Sigma_t \in \mathbb{R}^{d_\mu \times d_\mu}$$
- 8 Reorder variables in \tilde{x}_t to restore the variable ordering of (4).
- 9 **return** μ_t, Σ_t .

Algorithm 7: Dynamic EKF, State Propagation Sub-block.

Data: Current EKF state $\tilde{x}_t \in \mathbb{R}^{d_\mu}$, with mean $\bar{\mu}_t$ and covariance $\bar{\Sigma}_t$, (discrete-time) dynamics map $g: \mathbb{R}^{d_x} \rightarrow \mathbb{R}^{d_x}$.

Result: Propagated EKF state mean $\mu_{t+1} \in \mathbb{R}^{d_\mu}$ and covariance $\Sigma_{t+1} \in \mathbb{R}^{d_\mu \times d_\mu}$

- 1 $(\bar{\mu}_{t,x}, \bar{\mu}_{t,e}) \leftarrow \bar{\mu}_t$, with $\bar{\mu}_{t,x} \in \mathbb{R}^{d_x} :=$ ego robot pose mean.
- 2 $\begin{bmatrix} \bar{\Sigma}_{t,xx} & \bar{\Sigma}_{t,xe} \\ \bar{\Sigma}_{t,ex} & \bar{\Sigma}_{t,ee} \end{bmatrix} \leftarrow \bar{\Sigma}_t$, with $\bar{\Sigma}_{t,xx} \in \mathbb{R}^{d_x \times d_x} :=$ ego robot pose covariance.
- 3 $G_t \leftarrow \frac{\partial g}{\partial x} \Big|_{\bar{\mu}_{t,x}} \in \mathbb{R}^{d_x \times d_x}$.
- 4 $\mu_{t+1} \leftarrow (g(\bar{\mu}_{t,x}), \bar{\mu}_{t,e}) \in \mathbb{R}^{d_\mu}$.
- 5 $\Sigma_{t+1} \leftarrow \begin{bmatrix} G_t \bar{\Sigma}_{t,xx} G_t^\top + \Sigma_w & G_t \bar{\Sigma}_{t,xe} \\ \bar{\Sigma}_{t,ex} G_t^\top & \bar{\Sigma}_{t,ee} \end{bmatrix} \in \mathbb{R}^{d_\mu \times d_\mu}$.
- 6 **return** μ_{t+1}, Σ_{t+1} .

- [12] S. Leutenegger, S. Lynen, M. Bosse, R. Siegwart, and P. Furgale. “Keyframe-based Visual-Inertial Odometry using Nonlinear Optimization”. In: *IJRR* 34 (2015), pp. 314–334.
- [13] Kevin Doherty, David Baxter, Edward Schneeweiss, and John Leonard. “Probabilistic Data Association via Mixture Models for Robust Semantic SLAM”. In: May 2020, pp. 1098–1104. DOI: 10.1109/ICRA40945.2020.9197382.
- [14] Ming Hsiao and Michael Kaess. “MH-iSAM2: Multi-hypothesis iSAM using Bayes Tree and Hypo-tree”. In: *2019 International Conference on Robotics and Automation (ICRA)* (2019), pp. 1274–1280.
- [15] David Fridovich-Keil, Ellis Ratner, Lasse Peters, Anca D. Dragan, and Claire J. Tomlin. “Efficient Iterative Linear-Quadratic Approximations for Nonlinear Multi-Player General-Sum Differential Games”. In: *2020 IEEE International Conference on Robotics and Automation (ICRA)*, 2020, pp. 1475–1481. DOI: 10.1109/ICRA40945.2020.9197129.
- [16] F. Laine, D. Fridovich-Keil, C.Y. Chiu, and C.J. Tomlin. “The Computation of Approximate Generalized Feedback Nash Equilibria”. In: *arXiv* (2021).
- [17] J. Solà. “Simultaneous Localization and Mapping with the Extended Kalman Filter”. In: 2014. eprint: 1803.11288.
- [18] Asen L. Dontchev and Rockafellar R. Tyrrell. *Implicit Functions and Solution Mappings: A View from Variational Analysis*. Springer Science Business Media, LLC, 2009. ISBN: 978-0-387-87820-1.
- [19] John M. Lee. “Introduction to Smooth Manifolds”. In: (2000).

APPENDIX

The ArXiV version of this paper, which contains the appendix, is found here: <http://arxiv.org/abs/2207.05043>. The author will ensure that the link stays active.

The following supplementary material includes the appendix, which contains proofs and figures omitted in the main paper due to space limitations.

A. Proofs of Main Theorems

Theorem A.1: The feature augmentation step of standard dynamic EKF SLAM (Alg. 3) is equivalent to applying a Gauss-Newton step to $c_{dEKF,t,1} : \mathbb{R}^{d_\mu + N'_f d_f} \rightarrow \mathbb{R}$, with:

$$c_{dEKF,t,1}(\tilde{x}_t, f_{n_f+N_f+1}, \dots, f_{n_f+N_f+n'_f+N'_f}) \\ := \|\tilde{x}_t - \mu_t\|_{\Sigma_t^{-1}}^2 + \sum_{k=n_f+N_f+1}^{N_f+N'_f} \|z_{t,k} - h(x_t, f_k)\|_{\tilde{\Sigma}_v^{-1}}^2.$$

Proof: The proof parallels that of [1], Theorem 5.1, and is reproduced below for completeness.

By assumption, $\frac{\partial h}{\partial f_k}$ is surjective throughout the domain of h . Thus, by Theorem A.6, given any $x_t \in \mathbb{R}^{d_x}$ and $f_k \in \mathbb{R}^{d_f}$, there exists a local *inverse observation map* $\ell : U_x \times U_z \rightarrow U_f$, where $U_x \subset \mathbb{R}^{d_x}$, $U_f \subset \mathbb{R}^{d_f}$, and $U_z \subset \mathbb{R}^{d_z}$ are open neighborhoods of x_t , f_k , and $h(x_t, f_k)$, such that $h(x_t, \ell(x_t, z_t)) = z_t$ for each $x_t \in U_x$, $z_t \in U_z$, and $L_z = \tilde{H}_{t,f}^\dagger$, where $L_z := \frac{\partial \ell}{\partial z_t}(x_t, z_t) \in \mathbb{R}^{d_f \times d_z}$ and $\tilde{H}_{t,f} := \frac{\partial h}{\partial f_k}(x_t, f_k) \in \mathbb{R}^{d_z \times d_f}$, and \dagger denotes the Moore-Penrose pseudoinverse. Intuitively, ℓ directly generates position estimates of new features from their feature measurements and the current pose, by effectively “inverting” the measurement map $h : \mathbb{R}^{d_x} \times \mathbb{R}^{d_f} \rightarrow \mathbb{R}^{d_z}$ [17].

First, to simplify notation, define:

$$z_{t,new} = (z_{t,n_f+N_f+1}, \dots, z_{t,new}) \in \mathbb{R}^{(n'_f+N'_f)d_z}, \\ f_{t,new} = (f_{t,n_f+N_f+1}, \dots, f_{t,new}) \in \mathbb{R}^{(n'_f+N'_f)d_f}, \\ \tilde{h}(x_t, f_{t,new}) := (h(x_t, f_{t,n_f+N_f+1}), \dots, h(x_t, f_{t,new})) \\ \in \mathbb{R}^{(n'_f+N'_f)d_z}, \\ \tilde{\Sigma}_v = \text{diag}\{\Sigma_v, \dots, \Sigma_v\} \in \mathbb{R}^{(n'_f+N'_f)d_z \times (n'_f+N'_f)d_z}.$$

We can now rewrite the cost $c_{dEKF,t,1}$ as:

$$c_{dEKF,t,1}(\tilde{x}_t, f_{t,new}) \\ = \|\tilde{x}_t - \mu_t\|_{\Sigma_t^{-1}}^2 + \|\tilde{z}_{t,new} - \tilde{h}(x_t, f_{t,new})\|_{\tilde{\Sigma}_v^{-1}}^2.$$

To apply a Gauss-Newton step, we will define $C_1(\tilde{x}_t, f_{t,new})$ of an appropriate dimension such that $c_{dEKF,t,1}(\tilde{x}_t, f_{t,new}) = \|C_1(\tilde{x}_t, f_{t,new})\|_2^2$. A natural choice is furnished by $C_1(\tilde{x}_t, f_{t,new}) \in \mathbb{R}^{d_\mu + N_f d_f + N'_f d_z}$, as defined below:

$$C_1(\tilde{x}_t, f_{t,new}) \\ := \begin{bmatrix} \Sigma_t^{-1/2}(\tilde{x}_t - \mu_t) \\ \Sigma_v^{-1/2}(z_{t,new} - \tilde{h}(x_t, f_{t,new})) \end{bmatrix}.$$

Thus, our parameters for the Gauss-Newton algorithm submodule are:

$$\tilde{x}_t^* := (x_t^*, f_{t,1:n_f+N_f}^*, f_{t,new}^*) \\ = (\bar{\mu}_t, \ell(x_t^*, z_{t,n_f+N_f+1}), \dots, \ell(x_t^*, z_{t,new})) \\ \in \mathbb{R}^{d_x + (n_f + N_f + n'_f + N'_f)d_f},$$

where $x_t^* \in \mathbb{R}^{d_x}$, $f_{t,1:N_f}^* \in \mathbb{R}^{(n_f + N_f)d_f}$, $f_{t,new}^* \in \mathbb{R}^{(n'_f + N'_f)d_f}$, and:

$$C_1(\tilde{x}_t^*) = \begin{bmatrix} \Sigma_t^{-1/2}(\tilde{x}_t^* - \mu_t) \\ \tilde{\Sigma}_v^{-1/2}(z_{t,new} - \tilde{h}(x_t^*, f_{t,new}^*)) \end{bmatrix} \\ = \begin{bmatrix} 0 \\ 0 \end{bmatrix} \in \mathbb{R}^{d_\mu + (n'_f + N'_f)d_z}, \\ J = \begin{bmatrix} \Sigma_t^{-1/2} & O \\ -\tilde{\Sigma}_v^{-1/2} \tilde{H}_{t,x} [I_{d_x} \ O] & -\tilde{\Sigma}_v^{-1/2} \tilde{H}_{t,f} \end{bmatrix} \\ \in \mathbb{R}^{(d_\mu + (n'_f + N'_f)d_z) \times (d_x + (n'_f + N'_f)d_f)},$$

where $\tilde{H}_t := [\tilde{H}_{t,x} \ \tilde{H}_{t,f}] \in \mathbb{R}^{(n'_f + N'_f)d_z \times (d_x + (n'_f + N'_f)d_f)}$ is defined as the Jacobian of $\tilde{h} : \mathbb{R}^{d_x} \times \mathbb{R}^{(n'_f + N'_f)d_f} \rightarrow \mathbb{R}^{(n'_f + N'_f)d_z}$ at $(x_t^*, f_{t,new}^*) \in \mathbb{R}^{d_x + (n'_f + N'_f)d_f}$, with $\tilde{H}_{t,x} \in \mathbb{R}^{(n'_f + N'_f)d_z \times d_x}$ and $\tilde{H}_{t,f} \in \mathbb{R}^{(n'_f + N'_f)d_z \times (n'_f + N'_f)d_f}$. By [1], Algorithm 4.1, the Gauss-Newton update is thus given by:

$$\Sigma_t \\ \leftarrow (J^\top J)^\dagger \quad (8)$$

$$= \left(\begin{bmatrix} \Sigma_t^{-1/2} & -[I_{d_z}] \tilde{H}_{t,x}^\top \tilde{\Sigma}_v^{-1/2} \\ O & -\tilde{\Sigma}_v^{-1/2} \tilde{H}_{t,f} \end{bmatrix} \right. \\ \left. \cdot \begin{bmatrix} \Sigma_t^{-1/2} & O \\ -\tilde{\Sigma}_v^{-1/2} \tilde{H}_{t,x} [I_{d_x} \ O] & -\tilde{\Sigma}_v^{-1/2} \tilde{H}_{t,f} \end{bmatrix} \right)^\dagger \quad (9)$$

$$= \begin{bmatrix} \Omega_{t,xx} + \tilde{H}_{t,x}^\top \tilde{\Sigma}_v^{-1} \tilde{H}_{t,x} & \Omega_{t,xe} & \tilde{H}_{t,x}^\top \tilde{\Sigma}_v^{-1} \tilde{H}_{t,f} \\ \Omega_{t,ex} & \Omega_{t,ee} & O \\ \tilde{H}_{t,f}^\top \tilde{\Sigma}_v^{-1} \tilde{H}_{t,x} & O & \tilde{H}_{t,f}^\top \tilde{\Sigma}_v^{-1} \tilde{H}_{t,f} \end{bmatrix}^\dagger, \quad (10)$$

$$\bar{\mu}_t \leftarrow \tilde{x}_t^* - (J^\top J)^\dagger J^\top C_1(\tilde{x}_t^*) \\ = (\bar{\mu}_t, \ell(x_t^*, z_{t,n_f+N_f+1}), \dots, \ell(x_t^*, z_{t,new})),$$

where \dagger denotes the Moore-Penrose pseudoinverse.

Here, we have defined $\Omega_{t,xx} \in \mathbb{R}^{d_x \times d_x}$, $\Omega_{t,xe} = \Omega_{t,ex}^\top \in \mathbb{R}^{d_x \times d_z}$ and $\Omega_{t,ee} \in \mathbb{R}^{d_z \times d_z}$ by:

$$\begin{bmatrix} \Omega_{t,xx} & \Omega_{t,xe} \\ \Omega_{t,ex} & \Omega_{t,ee} \end{bmatrix} := \begin{bmatrix} \Sigma_{t,xx} & \Sigma_{t,xe} \\ \Sigma_{t,ex} & \Sigma_{t,ee} \end{bmatrix}^{-1} \\ \in \mathbb{R}^{(d_\mu + (n'_f + N'_f)d_f) \times (d_\mu + (n'_f + N'_f)d_f)} \quad (11)$$

To conclude the proof, we must show that (10) is identical to the update equations for covariance matrix in the standard formulation of the Extended Kalman Filter algorithm, i.e., we must show that:

$$\begin{bmatrix} \Sigma_{t,xx} & \Sigma_{t,xe} & \Sigma_{t,xx} L_x^\top \\ \Sigma_{t,ex} & \Sigma_{t,ee} & \Sigma_{t,ex} L_x^\top \\ L_x \Sigma_{t,xx} & L_x \Sigma_{t,xe} & L_x \Sigma_{t,xx} L_x^\top + L_z \Sigma_v L_z^\top \end{bmatrix} \\ = \begin{bmatrix} \Omega_{t,xx} + \tilde{H}_{t,x}^\top \tilde{\Sigma}_v^{-1} \tilde{H}_{t,x} & \Omega_{t,xe} & \tilde{H}_{t,x}^\top \tilde{\Sigma}_v^{-1} \tilde{H}_{t,f} \\ \Omega_{t,ex} & \Omega_{t,ee} & O \\ \tilde{H}_{t,f}^\top \tilde{\Sigma}_v^{-1} \tilde{H}_{t,x} & O & \tilde{H}_{t,f}^\top \tilde{\Sigma}_v^{-1} \tilde{H}_{t,f} \end{bmatrix}^\dagger$$

This follows by applying (11), the fact that $L_z = \tilde{H}_{t,f}^\dagger$, as well as the matrix equalities resulting from taking the derivative of the equation $z_t := h(x_t, \ell(x_t, z_t))$ with respect to $x_t \in \mathbb{R}^{d_x}$ and $z_t \in \mathbb{R}^{d_z}$, respectively:

$$I_{d_z} = \tilde{H}_{t,f} L_z,$$

$$O = \tilde{H}_{t,x} + H_{t,f} L_x.$$

We thus have:

$$\begin{aligned} & J^\top J \\ &= \begin{bmatrix} \Sigma_t^{-1/2} & -\begin{bmatrix} O \\ -\tilde{G}_f^o \top \\ I_{d_f} \end{bmatrix} \tilde{\Sigma}_\xi^{-1/2} \\ O & -\tilde{G}_f^o \top \tilde{\Sigma}_\xi^{-1/2} \end{bmatrix} \\ &\quad \cdot \begin{bmatrix} \Sigma_t^{-1/2} \\ -\tilde{\Sigma}_\xi^{-1/2} \begin{bmatrix} O & -\tilde{G}_f^o & I_{d_f} \end{bmatrix} & O \\ -\tilde{\Sigma}_\xi^{-1/2} \tilde{G}_f^o & \end{bmatrix} \\ &= \begin{bmatrix} \Sigma_t^{-1} + \begin{bmatrix} O \\ -\tilde{G}_f^o \top \\ I_{d_f} \end{bmatrix} \tilde{\Sigma}_\xi^{-1/2} \begin{bmatrix} O & -\tilde{G}_f^o \top & I_{d_f} \end{bmatrix} & \begin{bmatrix} O \\ -\tilde{G}_f^o \top \\ I_{d_f} \end{bmatrix} \tilde{\Sigma}_\xi^{-1} \tilde{G}_f^o \\ G_\xi^o \top \tilde{\Sigma}_\xi^{-1} \begin{bmatrix} O & -\tilde{G}_f^o & I_{d_f} \end{bmatrix} & \begin{bmatrix} G_\xi^o \top \tilde{\Sigma}_\xi^{-1} \tilde{G}_f^o \\ G_\xi^o \top \tilde{\Sigma}_\xi^{-1} G_\xi^o \end{bmatrix} \end{bmatrix}, \\ &= \begin{bmatrix} \Omega_{t,ee} & \Omega_{t,ef} & \Omega_{t,ef'} & O \\ \Omega_{t,fe} & \Omega_{t,ff} + \tilde{G}_f^o \top \tilde{\Sigma}_\xi^{-1} \tilde{G}_f^o & \Omega_{t,ff'} - \tilde{G}_f^o \top \tilde{\Sigma}_\xi^{-1} & \tilde{G}_f^o \top \tilde{\Sigma}_\xi^{-1} \tilde{G}_f^o \\ \Omega_{t,f'e} & \Omega_{t,f'f} - \tilde{\Sigma}_\xi^{-1} \tilde{G}_f^o & \Omega_{t,f'f'} + \tilde{\Sigma}_\xi^{-1} & -\tilde{\Sigma}_\xi^{-1} \tilde{G}_f^o \\ O & \tilde{G}_f^o \top \tilde{\Sigma}_\xi^{-1} \tilde{G}_f^o & -\tilde{G}_f^o \top \tilde{\Sigma}_\xi^{-1} & \tilde{G}_f^o \top \tilde{\Sigma}_\xi^{-1} G_\xi^o \end{bmatrix}, \end{aligned}$$

where we have defined:

$$\begin{bmatrix} \Omega_{t,ee} & \Omega_{t,ef} & \Omega_{t,ef'} \\ \Omega_{t,fe} & \Omega_{ff} & \Omega_{ff'} \\ \Omega_{t,f'e} & \Omega_{t,f'f} & \Omega_{t,f'f'} \end{bmatrix} := \Sigma_t^{-1} \in \mathbb{R}^{d_\mu \times d_\mu},$$

with $\Omega_{t,ff}, \Omega_{t,f'f'} \in \mathbb{R}^{N_f d_f \times N_f d_f}$. The Gauss-Newton update ([1], Algorithm 3) now gives:

$$\begin{aligned} & \Sigma_t \leftarrow (J^\top J)^\dagger \\ &= \begin{bmatrix} \Sigma_{t,ee} & \Sigma_{t,ef} & \Sigma_{t,ef'} & \Sigma_{t,\xi e}^\top \\ \Sigma_{t,fe} & \Sigma_{t,ff} & \Sigma_{t,ff'} & \Sigma_{t,\xi f}^\top \\ \Sigma_{t,f'e} & \Sigma_{t,f'f} & \Sigma_{t,f'f'} & \Sigma_{t,\xi f'}^\top \\ \Sigma_{t,\xi e} & \Sigma_{t,\xi f} & \Sigma_{t,\xi f'} & \Sigma_{t,\xi \xi} \end{bmatrix} \in \mathbb{R}^{d_\mu \times d_\mu} \end{aligned}$$

where:

$$\begin{bmatrix} \Sigma_{t,ee} & \Sigma_{t,ef} & \Sigma_{t,ef'} \\ \Sigma_{t,fe} & \Sigma_{t,ff} & \Sigma_{t,ff'} \\ \Sigma_{t,f'e} & \Sigma_{t,f'f} & \Sigma_{t,f'f'} \end{bmatrix} = \Sigma_t,$$

with $\Sigma_{t,ff}, \Sigma_{t,f'f'} \in \mathbb{R}^{N_f d_f \times N_f d_f}$, and:

$$\begin{aligned} \Sigma_{t,\xi e} &:= \tilde{\Gamma}_1 \Sigma_{t,fe} + \tilde{\Gamma}_2 \Sigma_{t,f'e} \in \mathbb{R}^{n_o d_x \times (d_\mu - 2N_f d_f)}, \\ \Sigma_{t,\xi f} &:= \tilde{\Gamma}_1 \Sigma_{t,ff} + \tilde{\Gamma}_2 \Sigma_{t,f'f} \in \mathbb{R}^{n_o d_x \times N_f d_f}, \\ \Sigma_{t,\xi f'} &:= \tilde{\Gamma}_1 \Sigma_{t,f'f'} + \tilde{\Gamma}_2 \Sigma_{t,f'f'} \in \mathbb{R}^{n_o d_x \times N_f d_f}, \\ \Sigma_{t,\xi \xi} &:= \tilde{\Gamma}_1 \Sigma_{t,ff} \tilde{\Gamma}_1^\top + \tilde{\Gamma}_2 \Sigma_{t,f'f} \tilde{\Gamma}_1^\top + \tilde{\Gamma}_1 \Sigma_{t,f'f'} \tilde{\Gamma}_2^\top \\ &\quad + \tilde{\Gamma}_2 (\Sigma_{t,f'f'} + \tilde{\Sigma}_\xi) \tilde{\Gamma}_2^\top \in \mathbb{R}^{n_o d_x \times n_o d_x} \end{aligned}$$

Theorem A.3: The static feature update step of standard dynamic EKF SLAM (Alg. 5) is equivalent to applying a Gauss-Newton step to $c_{dEKF,t,5} : \mathbb{R}^{d_\mu + N_f' d_f} \rightarrow \mathbb{R}$, with:

$$\begin{aligned} & c_{dEKF,t,5}(\tilde{x}_t, f_{n_f+1}, \dots, f_{n_f+n_f'}) \\ &:= \|\tilde{x}_t - \mu_t\|_{\Sigma_t^{-1}}^2 + \sum_{k=1}^{n_f} \|z_{t,k}^{(s)} - h(x_t, f_k^{(s)})\|_{\Sigma_v^{-1}}^2. \end{aligned}$$

Proof: The proof parallels that of [1], Theorem 5.2, and is reproduced below for completeness.

First, to simplify notation, define:

$$z_t := (z_{t,1}, \dots, z_{t,n_f}) \in \mathbb{R}^{n_f d_z},$$

$$\begin{aligned} f^{(s)} &:= (f_1^{(s)}, \dots, f_{n_f}^{(s)}) \in \mathbb{R}^{n_f d_f}, \\ \tilde{h}(x_t, f^{(s)}) &:= (h(x_t, f_1^{(s)}), \dots, h(x_t, f_{n_f}^{(s)})) \in \mathbb{R}^{n_f d_z}, \\ \tilde{\Sigma}_v &:= \text{diag}\{\Sigma_v, \dots, \Sigma_v\} \in \mathbb{R}^{n_f d_z \times n_f d_z}. \end{aligned}$$

We can then rewrite the cost as:

$$c_{dEKF,t,5}(\tilde{x}_t) = \|\tilde{x}_t^* - \mu_t\|_{\Sigma_t^{-1}}^2 + \|z_t - \tilde{h}(\tilde{x}_t^*)\|_{\tilde{\Sigma}_v^{-1}}^2.$$

To apply a Gauss-Newton step, we seek a vector $C_3(\tilde{x}_t)$ of an appropriate dimension such that $c_{dEKF,t,2}(\tilde{x}_t) = C_3(\tilde{x}_t)^\top C_3(\tilde{x}_t)$. A natural choice is furnished by $C_3(\tilde{x}_t) \in \mathbb{R}^{d_\mu + n_f d_z}$, as defined below:

$$C_3(\tilde{x}_t) := \begin{bmatrix} \Sigma_t^{-1/2}(\tilde{x}_t - \mu_t) \\ \tilde{\Sigma}_v^{-1/2}(z_t - \tilde{h}(\tilde{x}_t)) \end{bmatrix}.$$

Thus, our parameters for the Gauss-Newton algorithm submodule are:

$$\begin{aligned} \tilde{x}_t^* &= \mu_t \in \mathbb{R}^{d_\mu}, \\ C_3(\tilde{x}_t^*) &= \begin{bmatrix} \Sigma_t^{-1/2}(\tilde{x}_t^* - \mu_t) \\ \tilde{\Sigma}_v^{-1/2}(z_t - \tilde{h}(\tilde{x}_t^*)) \end{bmatrix} = \begin{bmatrix} 0 \\ \tilde{\Sigma}_v^{-1/2}(z_t - \tilde{h}(\mu_t)) \end{bmatrix} \\ &\in \mathbb{R}^{d_\mu + n_f d_z}, \\ J &= \begin{bmatrix} \Sigma_t^{-1/2} \\ -\tilde{\Sigma}_v^{-1/2} [H_t \quad O] \end{bmatrix} \in \mathbb{R}^{(d_\mu + n_f d_z) \times d_\mu}, \end{aligned}$$

where $\tilde{H}_t \in \mathbb{R}^{n_f d_z \times \mathbb{R}^{d_x + n_f d_f}}$ is defined as the Jacobian of $\tilde{h} : \mathbb{R}^{d_x} \times \mathbb{R}^{n_f d_f} \rightarrow \mathbb{R}^{n_f d_z}$ at $\tilde{x}_t^* \in \mathbb{R}^{d_\mu}$. By [1], Algorithm 4.1, the Gauss-Newton update is thus given by:

$$\begin{aligned} \bar{\Sigma}_t &\leftarrow (J^\top J)^{-1} \\ &= \left(\Sigma_t^{-1} + \begin{bmatrix} H_t^\top \\ O \end{bmatrix} \tilde{\Sigma}_v [H_t \quad O] \right)^{-1} \\ &= \Sigma_t - \Sigma_t \begin{bmatrix} H_t^\top \\ O \end{bmatrix} \left(\tilde{\Sigma}_v^{-1} + [H_t \quad O] \Sigma_t \begin{bmatrix} H_t^\top \\ O \end{bmatrix} \right)^{-1} \\ &\quad \cdot [H_t \quad O] \Sigma_t, \\ \bar{\mu}_t &\leftarrow \mu_t - (J^\top J)^{-1} J^\top C_3(\tilde{x}_t^*) \\ f &= \mu_t - (\Sigma_t^{-1} + H_t^\top \tilde{\Sigma}_v^{-1} H_t)^{-1} \begin{bmatrix} \Sigma_t^{-1/2} & -H_t^\top \tilde{\Sigma}_v^{-1/2} \\ 0 & \tilde{\Sigma}_v^{-1/2}(z_t - \tilde{h}(\mu_t)) \end{bmatrix} \\ &= \mu_t + (\Sigma_t^{-1} + H_t^\top \tilde{\Sigma}_v^{-1} H_t)^{-1} H_t^\top \tilde{\Sigma}_v^{-1}(z_t - \tilde{h}(\mu_t)), \\ &= \mu_t + \tilde{\Sigma}_v^{-1} \begin{bmatrix} H_t^\top \\ O \end{bmatrix} \left([H_t \quad O] \Sigma_t \begin{bmatrix} H_t^\top \\ O \end{bmatrix} + \tilde{\Sigma}_v \right)^{-1} \\ &\quad \cdot (z_t - \tilde{h}(\mu_t)), \end{aligned}$$

which are identical to the feature update equations for the mean and covariance matrix in the Extended Kalman Filter algorithm, i.e. (4) and (5) respectively. Note that, in the final step, we have used a variant of the Woodbury Matrix Identity. \blacksquare

Theorem A.4: The smoothing update step of standard dynamic EKF SLAM (Alg. 6) is equivalent to applying a Gauss-Newton step to $c_{dEKF,t,7} : \mathbb{R}^{d_\mu} \rightarrow \mathbb{R}$, with:

$$c_{dEKF,t,7}(\tilde{x}_t)$$

$$:= \|\tilde{x}_t - \mu_t\|_{\Sigma_t^{-1}}^2 + \sum_{\alpha=1}^{n_o} \|s(\xi_{t-2,\alpha}, \xi_{t-1,\alpha}, \xi_{t,\alpha})\|_{\tilde{\Sigma}_s^{-1}}^2.$$

Proof:

To simplify notation, define:

$$\begin{aligned} \xi_\tau &:= (\xi_{\tau,1}, \dots, \xi_{\tau,n_o}) \in \mathbb{R}^{n_o d_x}, \quad \forall \tau \in \{t-2, t-1, t\}, \\ \tilde{\Sigma}_s &:= \text{diag}\{\Sigma_s, \dots, \Sigma_s\} \in \mathbb{R}^{n_o d_x \times n_o d_x}. \end{aligned}$$

We can then rewrite the cost as:

$$\begin{aligned} c_{dEKF,t,7}(\tilde{x}_t) &:= \|\tilde{x}_t - \mu_t\|_{\Sigma_t^{-1}}^2 + \|s(\xi_{t-2}, \xi_{t-1}, \xi_t)\|_{\tilde{\Sigma}_s^{-1}}^2. \end{aligned}$$

To apply a Gauss-Newton step, we must find a vector $C_4(\tilde{x}_t)$, of appropriate dimension, such that $c_{dEKF,t,7} = \|C_4(\tilde{x}_t)\|_2^2$. To this end, define:

$$C_4(\tilde{x}_t) := \begin{bmatrix} \Sigma_t^{-1/2}(\tilde{x}_t - \bar{\mu}_t) \\ \tilde{\Sigma}_s^{-1/2} s(\xi_{t-2}, \xi_{t-1}, \xi_t) \end{bmatrix} \in \mathbb{R}^{d_\mu + d_x}.$$

The Gauss-Newton submodule parameters are therefore:

$$\begin{aligned} \tilde{x}_t^* &= \mu_t \in \mathbb{R}^{d_x + n_f d_f}, \\ C_4(\tilde{x}_t^*) &= \begin{bmatrix} \Sigma_t^{-1/2}(\tilde{x}_t^* - \bar{\mu}_t) \\ s(\xi_{t-2}, \xi_{t-1}, \xi_t) \end{bmatrix} \\ &\in \mathbb{R}^{d_x + n_f d_f + n_f d_z}, \\ J &= \begin{bmatrix} O & \Sigma_t^{-1/2} S_{t-2} & \tilde{\Sigma}_s^{-1/2} S_{t-1} & \tilde{\Sigma}_s^{-1/2} S_t \end{bmatrix} \\ &\in \mathbb{R}^{(d_\mu + d_x) \times d_\mu}, \end{aligned}$$

and thus:

$$\begin{aligned} J^\top J &= \begin{bmatrix} O \\ \Sigma_t^{-1/2} S_{t-2}^\top \tilde{\Sigma}_s^{-1/2} \\ S_{t-1}^\top \tilde{\Sigma}_s^{-1/2} \\ S_t^\top \tilde{\Sigma}_s^{-1/2} \end{bmatrix} \\ &\quad \cdot \begin{bmatrix} \Sigma_t^{-1/2} \\ O & \tilde{\Sigma}_s^{-1/2} S_{t-2} & \tilde{\Sigma}_s^{-1/2} S_{t-1} & \tilde{\Sigma}_s^{-1/2} S_t \end{bmatrix} \\ &= \Sigma_t^{-1} + \begin{bmatrix} O \\ S_{t-2}^\top \\ S_{t-1}^\top \\ S_t^\top \end{bmatrix} \tilde{\Sigma}_s^{-1} [O \quad S_{t-2} \quad S_{t-1} \quad S_t] \end{aligned}$$

By [1], Algorithm 4.1, the Gauss-Newton update is given by:

$$\begin{aligned} \Sigma_t &\leftarrow (J^\top J)^{-1} \\ &= \left(\Sigma_t^{-1} + \begin{bmatrix} O \\ S_{t-2}^\top \\ S_{t-1}^\top \\ S_t^\top \end{bmatrix} \tilde{\Sigma}_s^{-1} [O \quad S_{t-2} \quad S_{t-1} \quad S_t] \right)^{-1} \\ &= \Sigma_t - \Sigma_t \begin{bmatrix} O \\ S_{t-2}^\top \\ S_{t-1}^\top \\ S_t^\top \end{bmatrix} \\ &\quad \cdot \begin{pmatrix} \tilde{\Sigma}_s + [O \quad S_{t-2} \quad S_{t-1} \quad S_t] \Sigma_t \begin{bmatrix} S_{t-2}^\top \\ S_{t-1}^\top \\ S_t^\top \end{bmatrix} \end{pmatrix}^{-1} \\ &\quad \cdot [O \quad S_{t-2} \quad S_{t-1} \quad S_t] \Sigma_t \end{aligned}$$

$$\begin{aligned}
\mu_t &\leftarrow \mu_t - (J^\top J)^{-1} J^\top C_4(\mu_t) \\
&= \mu_t - \left(\Sigma_t^{-1} + \begin{bmatrix} O \\ S_{t-2}^\top \\ S_{t-1}^\top \\ S_t^\top \end{bmatrix} \tilde{\Sigma}_s^{-1} [O \quad S_{t-2} \quad S_{t-1} \quad S_t] \right)^{-1} \\
&\quad \begin{bmatrix} O \\ \Sigma_t^{-1/2} \quad S_{t-2}^\top \tilde{\Sigma}_s^{-1/2} \\ S_{t-1}^\top \tilde{\Sigma}_s^{-1/2} \\ S_t^\top \tilde{\Sigma}_s^{-1/2} \end{bmatrix} \cdot \begin{bmatrix} O \\ \tilde{\Sigma}_s^{-1/2} s(\xi_{t-2}, \xi_{t-1}, \xi_t) \end{bmatrix} \\
&= \mu_t - \left(\Sigma_t^{-1} + \begin{bmatrix} O \\ S_{t-2}^\top \\ S_{t-1}^\top \\ S_t^\top \end{bmatrix} \tilde{\Sigma}_s^{-1} [O \quad S_{t-2} \quad S_{t-1} \quad S_t] \right)^{-1} \\
&\quad \cdot \begin{bmatrix} O \\ S_{t-2}^\top \\ S_{t-1}^\top \\ S_t^\top \end{bmatrix} \tilde{\Sigma}_s^{-1} s(\xi_{t-2}, \xi_{t-1}, \xi_t) \\
&= \mu_t - \Sigma_t \begin{bmatrix} O \\ S_{t-2}^\top \\ S_{t-1}^\top \\ S_t^\top \end{bmatrix} \\
&\quad \cdot \left(\tilde{\Sigma}_s + [O \quad S_{t-2} \quad S_{t-1} \quad S_t] \Sigma_t \begin{bmatrix} O \\ S_{t-2}^\top \\ S_{t-1}^\top \\ S_t^\top \end{bmatrix} \right)^{-1} \\
&\quad \cdot s(\xi_{t-2}, \xi_{t-1}, \xi_t)
\end{aligned}$$

via the Woodbury Matrix Identity. This establishes the equivalence between the smoothing update equations for the dynamic EKF algorithm as written in our optimization-based algorithm, and as written in the mold of the standard EKF SLAM algorithm [10]. \blacksquare

Theorem A.5: The state propagation step of standard dynamic EKF SLAM (Alg. 7) is equivalent to applying a Gauss-Newton step to $c_{dEKF,t,9} : \mathbb{R}^{d_\mu} \rightarrow \mathbb{R}$, with:

$$\begin{aligned}
c_{dEKF,t,9}(\tilde{x}_t, x_{t+1}) \\
:= \|\tilde{x}_t - \bar{\mu}_t\|_{\Sigma_t^{-1}}^2 + \|x_{t+1} - g(x_t)\|_{\Sigma_w^{-1}}^2.
\end{aligned}$$

Proof: The proof parallels that of [1], Theorem 5.3, and is reproduced below for completeness.

Intuitively, the state propagation step marginalizes out $x_t \in \mathbb{R}^{d_x}$ in the full state vector $\tilde{x}_t \in \mathbb{R}^{d_x}$, and retains $x_{t+1} \in \mathbb{R}^{d_x}$. In the notation of our Marginalization algorithm submodule:

$$\begin{aligned}
\tilde{x}_{t,K} &= (x_{t+1}, f^{(s)}, f^{(m)}, \xi) \in \mathbb{R}^{d_\mu}, \\
\tilde{x}_{t,M} &= x_t \in \mathbb{R}^{d_x},
\end{aligned}$$

with the costs:

$$\begin{aligned}
c_K(x_{t+1}) &= 0 \\
c_M(\tilde{x}_t, x_{t+1}) &= \|\tilde{x}_t - \bar{\mu}_t\|_{\Sigma_t^{-1}}^2 + \|x_{t+1} - g(x_t)\|_{\Sigma_w^{-1}}^2.
\end{aligned}$$

To apply a marginalization step, we must first define vectors $C_K(x_K) = C_K(\tilde{x}_t)$ and $C_M(x_K, x_M) = C_M(\tilde{x}_t, x_{t+1})$ of appropriate dimensions such that $c_{dEKF,t,9}(\tilde{x}_t, x_{t+1}) = C_K(x_{t+1})^\top C_K(x_{t+1}) + C_M(\tilde{x}_t, x_{t+1})^\top C_M(\tilde{x}_t, x_{t+1})$. To this end, we identify the following parameters, in the language of

a Marginalization step ([1], Section 2):

$$\begin{aligned}
C_K(\tilde{x}_{t,K}) &:= 0 \in \mathbb{R} \\
C_M(\tilde{x}_{t,K}, \tilde{x}_{t,M}) &:= \begin{bmatrix} \bar{\Sigma}_t^{-1/2}(\tilde{x}_t - \bar{\mu}_t) \\ \Sigma_w^{-1/2}(x_{t+1} - g(x_t)) \end{bmatrix} \in \mathbb{R}^{d_\mu + d_x}.
\end{aligned}$$

For convenience, we will define the pose and feature track components of the mean $\mu_t \in \mathbb{R}^{d_\mu}$ by $\mu_t := (\mu_{t,x}, \mu_{t,e}) \in \mathbb{R}^{d_\mu}$, with $\mu_{t,x} \in \mathbb{R}^{d_x}$. In addition, we will define the components of $\bar{\Sigma}_t^{-1/2} \in \mathbb{R}^{d_\mu \times d_\mu}$ and $\bar{\Sigma}_t^{-1} \in \mathbb{R}^{d_\mu \times d_\mu}$ by:

$$\begin{aligned}
\begin{bmatrix} \Omega_{t,xx} & \Omega_{t,xe} \\ \Omega_{t,ex} & \Omega_{t,ee} \end{bmatrix} &:= \bar{\Sigma}_t^{-1} \in \mathbb{R}^{d_\mu \times d_\mu}, \\
\begin{bmatrix} \Gamma_{t,xx} & \Gamma_{t,xe} \\ \Gamma_{t,ex} & \Gamma_{t,ee} \end{bmatrix} &:= \bar{\Sigma}_t^{-1/2} \in \mathbb{R}^{d_\mu \times d_\mu},
\end{aligned}$$

where $\Sigma_{t,xx}, \Gamma_{t,xx} \in \mathbb{R}^{d_x \times d_x}$. Using the above definitions, we can reorder the residuals in $C_K \in \mathbb{R}$ and $C_M \in \mathbb{R}^{d_\mu + d_x}$, and thus redefine them by:

$$\begin{aligned}
C_K(\tilde{x}_{t,K}) &= 0 \in \mathbb{R} \\
C_M(\tilde{x}_{t,K}, \tilde{x}_{t,M}) \\
&= \begin{bmatrix} \Gamma_{t,xx}(x_t - \mu_{t,x}) + \Gamma_{t,xe}(f^{(s)} - \mu_{t,f}) \\ \Sigma_w^{-1/2}(x_{t+1} - g(x_t)) \\ \Gamma_{t,ex}(x_t - \mu_{t,x}) + \Gamma_{t,ee}(f^{(s)} - \mu_{t,f}) \end{bmatrix} \in \mathbb{R}^{d_\mu + d_x}.
\end{aligned}$$

Our state variables and cost functions for the Gauss-Newton algorithm submodule are:

$$\begin{aligned}
\bar{x}_M^* &= \tilde{x}_t^* = \bar{\mu}_t \in \mathbb{R}^{d_\mu}, \\
\bar{x}_K^* &= g(\tilde{x}_t^*) = g(\bar{\mu}_t) \in \mathbb{R}^{d_\mu}, \\
C_K(\tilde{x}_{t,K}^*) &= 0 \in \mathbb{R}, \\
C_M(\tilde{x}_{t,K}^*, \tilde{x}_{t,M}^*) &= \begin{bmatrix} 0 \\ 0 \end{bmatrix} \in \mathbb{R}^{d_\mu + d_x}, \\
J_K &= \begin{bmatrix} O & \Gamma_{t,xe} \\ \Sigma_w^{-1/2} & O \\ O & \Gamma_{t,ee} \end{bmatrix} \in \mathbb{R}^{(d_\mu + d_x) \times d_\mu}, \\
J_M &= \begin{bmatrix} \Gamma_{t,xx} \\ -\Sigma_w^{-1/2} G_t \\ \Gamma_{t,ex} \end{bmatrix} \in \mathbb{R}^{(d_\mu + d_x) \times d_x},
\end{aligned}$$

where we have defined G_t to be the Jacobian of $g : \mathbb{R}^{d_x} \rightarrow \mathbb{R}^{d_x}$ at $\bar{\mu}_{t,x} \in \mathbb{R}^{d_x}$, i.e.:

$$G_t := \left. \frac{\partial g}{\partial x_t} \right|_{x_t=\bar{\mu}_{t,x}}$$

Applying the Marginalization equations, we thus have:

$$\begin{aligned}
\mu_{t+1} &\leftarrow \tilde{x}_{t,K} - \Sigma_{t+1} J_K^\top [I - J_M (J_M^\top J_M)^{-1} J_M^\top] \\
&\quad C_M(\bar{x}_K^*, \bar{x}_M^*) \\
&= g(\bar{\mu}_t), \\
\Sigma_{t+1} &\leftarrow (J_K^\top [I - J_M (J_M^\top J_M)^{-1} J_M^\top] J_K)^{-1}, \\
&= (J_K^\top J_K - J_K^\top J_M (J_M^\top J_M)^{-1} J_M^\top J_K)^{-1}, \\
&= \left(\begin{bmatrix} \Sigma_w^{-1} & O \\ O & \Gamma_{ex} \Gamma_{xe} + \Gamma_{ee}^2 \end{bmatrix} - \begin{bmatrix} -\Sigma_w^{-1} G_t \\ \Gamma_{ex} \Gamma_{xx} + \Gamma_{ee} \Gamma_{ex} \end{bmatrix} \right. \\
&\quad \left. (\Gamma_{xx}^2 + \Gamma_{xe} \Gamma_{ex} + G_t^\top \Sigma_w^{-1} G_t)^{-1} \right)
\end{aligned}$$

$$\begin{aligned}
& \cdot \begin{bmatrix} -G_t^\top \Sigma_w^{-1} & \Gamma_{xx} \Gamma_{xe} + \Gamma_{ex} \Gamma_{ee} \end{bmatrix} \begin{pmatrix} \Sigma_w^{-1} & O \\ O & \Omega_{ee} \end{pmatrix} - \begin{bmatrix} -\Sigma_w^{-1} G_t \\ \Omega_{ex} \end{bmatrix} \\
& = \left(\begin{bmatrix} \Sigma_w^{-1} & O \\ O & \Omega_{ee} \end{bmatrix} - \begin{bmatrix} -\Sigma_w^{-1} G_t \\ \Omega_{ex} \end{bmatrix} \right)^{-1} \left(\Omega_{xx} + G_t^\top \Sigma_w^{-1} G_t \right)^{-1} \begin{bmatrix} -G_t^\top \Sigma_w^{-1} & \Omega_{xe} \end{bmatrix}
\end{aligned}$$

To show that this is indeed identical to the propagation equation for the covariance matrix in the standard formulation of the dynamic Extended Kalman Filter algorithm, i.e. Algorithm 2, Line 5, we must show that:

$$\begin{aligned}
& \left(\begin{bmatrix} \Sigma_w^{-1} & O \\ O & \Omega_{ee} \end{bmatrix} - \begin{bmatrix} -\Sigma_w^{-1} G_t \\ \Omega_{ex} \end{bmatrix} \right) \left(\Omega_{xx} + G_t^\top \Sigma_w^{-1} G_t \right)^{-1} \\
& \quad \left[-G_t^\top \Sigma_w^{-1} \quad \Omega_{xe} \right]^{-1} \\
& = \begin{bmatrix} G_t \bar{\Sigma}_{t,xx} G_t^\top + \Sigma_w & G_t \bar{\Sigma}_{t,xe} \\ \bar{\Sigma}_{t,xe} G_t^\top & \bar{\Sigma}_{t,ee} \end{bmatrix}
\end{aligned}$$

This follows by brute-force expanding the above block matrix components, and applying Woodbury's Matrix Identity, along with the definitions of $\Sigma_{t,xx}$, $\Gamma_{t,xx}$, $\Sigma_{t,xe}$, $\Gamma_{t,xe}$, $\Sigma_{t,ex}$, $\Gamma_{t,ex}$, $\Sigma_{t,ee}$, and $\Gamma_{t,ee}$. \blacksquare

B. Auxiliary Theorems

For the proof of Theorem A.1 above, we require the following result, an extension of the classic Implicit Function Theorem and of [18], Theorem 1F.6. This result appears as Exercise 1F.9 in [18], and is presented here, with proof, for completeness.

Theorem A.6: Let $f : \mathbb{R}^n \times \mathbb{R}^d \rightarrow \mathbb{R}^p$ be a k -times continuously differentiable (i.e., C^k) function, with $p \leq d$. Fix $x^* \in \mathbb{R}^n$, $y^* \in \mathbb{R}^d$ arbitrarily, and let $z^* := f(x^*, y^*) \in \mathbb{R}^p$. Define $df_x := \frac{\partial f}{\partial x} \in \mathbb{R}^{p \times n}$ and $df_y := \frac{\partial f}{\partial y} \in \mathbb{R}^{p \times d}$ at each point in $\mathbb{R}^n \times \mathbb{R}^d$, the domain of f . If $df_y(x^*, y^*)$ is surjective, then there exists open neighborhoods $U_x \subset \mathbb{R}^n$, $U_y \subset \mathbb{R}^d$, and $U_z \subset \mathbb{R}^p$ of x^* , y^* , and z^* , respectively, and a C^k map $g : U_x \times U_z \rightarrow U_y$, such that:

- 1) $f(x, g(x, z)) = z$, $\forall x \in U_z$, $z \in U_z$.
- 2) $dg_x(x^*, z^*) = (-df_y^\top (df_y df_y^\top)^{-1} df_x(x^*, y^*))$, where $dg_x := \frac{\partial g}{\partial x}$ in the domain of g .

Proof: Define $\bar{f} : \mathbb{R}^n \times \mathbb{R}^k \rightarrow \mathbb{R}^n \times \mathbb{R}^p$ by $\bar{f}(x, y) := (x, f(x, y))$ for each $(x, y) \in \mathbb{R}^n \times \mathbb{R}^k$. Then $d\bar{f}_x := \frac{\partial \bar{f}}{\partial x}$ is surjective at (x^*, y^*) . Thus, by [18], Theorem 1F.6 (an extension of the Inverse Function Theorem), there exist open neighborhoods $U_x \subset \mathbb{R}^n$, $U_y \subset \mathbb{R}^d$, and $U_z \subset \mathbb{R}^p$ of x^* , y^* , and z^* , respectively, and a C^k map $\bar{g} : U_x \times U_z \rightarrow U_x \times U_y$, such that:

$$\begin{aligned}
\bar{f}(\bar{g}(x, z)) &= (x, z), \quad \forall (x, z) \in U_x \times U_z, \\
d\bar{g}_x(x^*, z^*) &= (-df_y^\top (df_y df_y^\top)^{-1} df_x(x^*, y^*)),
\end{aligned}$$

where $d\bar{g}_x := \frac{\partial \bar{g}}{\partial x}$ in the domain of \bar{g} .

Let the components of \bar{g} be given by $\bar{g}(x, z) := (g_1(x, z), g_2(x, z))$ for each $x \in U_x$, $z \in U_z$, with $g_1 :$

$U_x \times U_z \rightarrow U_x$ and $g_2 : U_x \times U_z \rightarrow U_y$. We claim that g_2 is our desired function. First, for each $x \in U_x$ and $z \in U_z$:

$$\begin{aligned}
(x, z) &= \bar{f}(\bar{g}(x, z)) = \bar{f}(g_1(x, z), g_2(x, z)) \\
&= (g_1(x, z), f(g_1(x, z), g_2(x, z))),
\end{aligned}$$

so $g_1(x, z) = x$, and thus, as desired:

$$(x, z) = (x, f(x, g_2(x, z)))$$

Next, let $df \in \mathbb{R}^{(n+p) \times k}$, $d\bar{f} \in \mathbb{R}^{(n+p) \times (n+k)}$, and $d\bar{g} \in \mathbb{R}^{(n+k) \times (n+p)}$ denote the (full) derivatives of the maps f , \bar{f} , and \bar{g} , in their respective domains. Then:

$$\begin{aligned}
& d\bar{g}(x^*, z^*) \\
&= (-df_y^\top (df_y df_y^\top)^{-1} df_x)(x^*, y^*) \\
&= \begin{bmatrix} I_{n \times n} & df_x^\top \\ O_{k \times n} & df_y^\top \end{bmatrix} \left(\begin{bmatrix} I_{n \times n} & O_{k \times n} \\ df_x & df_y \end{bmatrix} \begin{bmatrix} I_{n \times n} & df_x^\top \\ O_{k \times n} & df_y^\top \end{bmatrix} \right)^{-1} (x^*, y^*) \\
&= \begin{bmatrix} I_{n \times n} & df_x^\top \\ O_{k \times n} & df_y^\top \end{bmatrix} \left[df_x \quad df_x df_x^\top + df_y df_y^\top \right]^{-1} (x^*, y^*) \\
&= \begin{bmatrix} I_{n \times n} & O_{k \times n} \\ -df_y^\top (df_y df_y^\top)^{-1} df_x & df_y^\top (df_y df_y^\top)^{-1} \end{bmatrix} (x^*, y^*).
\end{aligned}$$

Consequently:

$$d\bar{g}(g_2)_x(x^*, z^*) = -df_y^\top (df_y df_y^\top)^{-1} df_x(x^*, y^*),$$

as desired. \blacksquare

For the proof of Theorem 4.1 above, we require the following results, derived from an corollary to the Global Rank Theorem ([19], Theorem 4.14).

Theorem A.7 (Corollary to [19], Theorem 4.14): Let \mathcal{M} and \mathcal{N} denote manifolds of dimension $d_{\mathcal{M}}$ and $d_{\mathcal{N}}$, respectively, with $d_{\mathcal{M}} \leq d_{\mathcal{N}}$, and let $f : \mathcal{M} \rightarrow \mathcal{N}$ be a smooth local injection about the point $p \in \mathcal{M}$. Then for any pair of smooth local charts $(U_{\mathcal{M}}, \phi_{\mathcal{M}})$, $(U_{\mathcal{N}}, \phi_{\mathcal{N}})$ centered at p and $f(p)$, respectively, where $U_{\mathcal{M}}, U_{\mathcal{N}}$ are open neighborhoods of p and $f(p)$ in \mathcal{M} and \mathcal{N} , respectively, with $f(U_{\mathcal{M}}) \subset U_{\mathcal{N}}$, there exists:

- 1) Open neighborhoods $U'_{\mathcal{M}} \subset U_{\mathcal{M}}$ and $U'_{\mathcal{N}} \subset U_{\mathcal{N}}$ of p and $f(p)$ in \mathcal{M} and \mathcal{N} , respectively, and
- 2) A local inverse map $g : U'_{\mathcal{N}} \rightarrow U'_{\mathcal{M}}$, such that $(g \circ f)(p') = p'$ for all $p' \in \mathcal{M}'$, and:

$$\frac{d}{dy^i} (\phi_{\mathcal{M}} \circ g \circ \phi_{\mathcal{N}}^{-1}) = \left(\frac{d}{dx^i} (\phi_{\mathcal{N}} \circ f \circ \phi_{\mathcal{M}}^{-1}) \right)^\dagger,$$

where (x^1, \dots, x^m) and (y^1, \dots, y^n) denote Euclidean coordinates in $\phi_{\mathcal{M}}(U'_{\mathcal{M}})$ and $\phi_{\mathcal{N}}(U'_{\mathcal{N}})$, respectively, and \dagger denotes the Moore-Penrose pseudoinverse.

Proof: By the Global Rank Theorem ([19], Theorem 4.14), there exists a pair of smooth local charts, $(\bar{U}_{\mathcal{M}}, \bar{\phi}_{\mathcal{M}})$ and $(\bar{U}_{\mathcal{N}}, \bar{\phi}_{\mathcal{N}})$, centered at p and $f(p)$, respectively, such that, for any $x := (x_1, \dots, x_m) \in \bar{\phi}_{\mathcal{M}}(\bar{U}_{\mathcal{M}})$:

$$(\bar{\phi}_{\mathcal{N}} \circ f \circ \bar{\phi}_{\mathcal{M}}^{-1})(x_1, \dots, x_m) = (x_1, \dots, x_m, 0, \dots, 0).$$

Define $\text{proj} : \bar{\phi}_{\mathcal{N}}(\bar{U}_{\mathcal{N}}) \rightarrow \bar{\phi}_{\mathcal{M}}(\bar{U}_{\mathcal{M}})$ by:

$$\text{embed}(x) := (x_1, \dots, x_m, 0, \dots, 0) \text{proj}(y) := (y_1, \dots, y_m),$$

for each $x := (x_1, \dots, x_m) \in \phi_{\mathcal{N}}(\overline{U}_{\mathcal{N}})$ and $y := (y_1, \dots, y_m, \dots, y_n) \in \phi_{\mathcal{M}}(\overline{U}_{\mathcal{M}})$.

Now, observe that:

$$\begin{aligned} & \phi_{\mathcal{N}} \circ f \circ \phi_{\mathcal{M}}^{-1} \\ &= (\phi_{\mathcal{N}} \circ \overline{\phi}_{\mathcal{N}}^{-1}) \circ (\overline{\phi}_{\mathcal{N}} \circ f \circ \overline{\phi}_{\mathcal{M}}^{-1}) \circ (\overline{\phi}_{\mathcal{M}} \circ \phi_{\mathcal{M}}^{-1}), \\ \Rightarrow & d(\phi_{\mathcal{N}} \circ f \circ \phi_{\mathcal{M}}^{-1}) \\ &= d(\phi_{\mathcal{N}} \circ \overline{\phi}_{\mathcal{N}}^{-1}) \circ d(\overline{\phi}_{\mathcal{N}} \circ f \circ \overline{\phi}_{\mathcal{M}}^{-1}) \circ d(\overline{\phi}_{\mathcal{M}} \circ \phi_{\mathcal{M}}^{-1}) \\ &= d(\phi_{\mathcal{N}} \circ \overline{\phi}_{\mathcal{N}}^{-1}) \circ \begin{bmatrix} I_{m \times m} \\ O_{(n-m) \times m} \end{bmatrix} \circ d(\overline{\phi}_{\mathcal{M}} \circ \phi_{\mathcal{M}}^{-1}), \end{aligned}$$

where $d(\cdot)$ denotes the Jacobian of a smooth map. Intuitively, we wish to take the pseudoinverse of the matrix near the “center” of the above expression. Since $d(\phi_{\mathcal{N}} \circ \overline{\phi}_{\mathcal{N}}^{-1})$ and $d(\overline{\phi}_{\mathcal{M}} \circ \phi_{\mathcal{M}}^{-1})$ are, in general, not orthogonal matrices, some additional processing is required. In particular, let $Q_{\mathcal{N}} R_{\mathcal{N}}$ and $Q_{\mathcal{M}} R_{\mathcal{M}}$ be the QR decomposition of $d(\phi_{\mathcal{N}} \circ \overline{\phi}_{\mathcal{N}}^{-1})$ and $d(\overline{\phi}_{\mathcal{M}} \circ \phi_{\mathcal{M}}^{-1})$, respectively, and define $g : U_{\mathcal{N}} \cap \overline{U}_{\mathcal{N}} \rightarrow U_{\mathcal{M}} \cap \overline{U}_{\mathcal{M}}$ by:

$$\begin{aligned} g := & \overline{\phi}_{\mathcal{M}}^{-1} \circ L_{R_{\mathcal{M}}^{-1}} \circ L_{(L_{R_{\mathcal{N}}} \circ \overline{\phi}_{\mathcal{N}} \circ f \circ \overline{\phi}_{\mathcal{M}}^{-1} \circ L_{R_{\mathcal{M}}^{-1}})^{\dagger}} \\ & \circ L_{R_{\mathcal{N}}} \circ \overline{\phi}_{\mathcal{N}} \end{aligned}$$

where, given any matrix $A \in \mathbb{R}^{m \times n}$, we use $L_A : \mathbb{R}^n \times \mathbb{R}^m$ to denote the corresponding linear map. Then:

$$\begin{aligned} & (g \circ f)(p) \\ &= (\overline{\phi}_{\mathcal{M}}^{-1} \circ L_{R_{\mathcal{M}}^{-1}} \circ (L_{R_{\mathcal{N}}} \circ \overline{\phi}_{\mathcal{N}} \circ f \circ \overline{\phi}_{\mathcal{M}}^{-1} \circ L_{R_{\mathcal{M}}^{-1}})^{\dagger} \\ & \quad \circ L_{R_{\mathcal{N}}} \circ \overline{\phi}_{\mathcal{N}}) \\ & \quad \circ (\overline{\phi}_{\mathcal{N}}^{-1} \circ L_{R_{\mathcal{N}}^{-1}} \circ L_{R_{\mathcal{N}}} \circ \overline{\phi}_{\mathcal{N}} \circ f \\ & \quad \circ \overline{\phi}_{\mathcal{M}}^{-1} \circ L_{R_{\mathcal{M}}^{-1}} \circ L_{R_{\mathcal{M}}} \circ \overline{\phi}_{\mathcal{M}})(p) \\ &= p, \end{aligned}$$

for any $p \in \mathcal{M}$, and:

$$\begin{aligned} & \left(\frac{d}{dx} (\phi_{\mathcal{N}} \circ f \circ \phi_{\mathcal{M}}^{-1}) \right)^{\dagger} \\ &= \left(L_{Q_{\mathcal{N}}} \circ L_{R_{\mathcal{N}}} \circ \text{embed} \circ L_{R_{\mathcal{M}}^{-1}} \circ L_{Q_{\mathcal{M}}^{-1}} \right)^{\dagger} \\ &= Q_{\mathcal{M}} \left(R_{\mathcal{N}} \begin{bmatrix} I_{m \times m} & O_{m \times (n-m)} \end{bmatrix} R_{\mathcal{M}}^{-1} \right)^{\dagger} Q_{\mathcal{N}}^{-1}, \end{aligned}$$

whereas:

$$\begin{aligned} & \frac{d}{dy} (\phi_{\mathcal{M}} \circ g \circ \phi_{\mathcal{N}}^{-1}) \\ &= \left(\phi_{\mathcal{M}} \circ \phi_{\mathcal{M}}^{-1} \circ L_{R_{\mathcal{M}}^{-1}} \right. \\ & \quad \left. \circ L_{(L_{R_{\mathcal{N}}} \circ \overline{\phi}_{\mathcal{N}} \circ f \circ \overline{\phi}_{\mathcal{M}}^{-1} \circ L_{R_{\mathcal{M}}^{-1}})^{\dagger}} \circ L_{R_{\mathcal{N}}} \right. \\ & \quad \left. \circ \overline{\phi}_{\mathcal{N}} \circ \phi_{\mathcal{N}}^{-1} \right) \\ &= Q_{\mathcal{M}} R_{\mathcal{M}} \\ & \quad \cdot R_{\mathcal{M}} \left(R_{\mathcal{N}} \begin{bmatrix} I_{m \times m} & O_{m \times (n-m)} \end{bmatrix} R_{\mathcal{M}}^{-1} \right)^{\dagger} R_{\mathcal{N}} \end{aligned}$$

$$\begin{aligned} & \cdot R_{\mathcal{N}}^{-1} Q_{\mathcal{N}}^{-1} \\ &= Q_{\mathcal{M}} \left(R_{\mathcal{N}} \begin{bmatrix} I_{m \times m} & O_{m \times (n-m)} \end{bmatrix} R_{\mathcal{M}}^{-1} \right)^{\dagger} Q_{\mathcal{N}}^{-1}, \end{aligned}$$

so we have:

$$\frac{d}{dy^i} (\phi_{\mathcal{M}} \circ g \circ \phi_{\mathcal{N}}^{-1}) = \left(\frac{d}{dx^i} (\phi_{\mathcal{N}} \circ f \circ \phi_{\mathcal{M}}^{-1}) \right)^{\dagger},$$

as claimed. \blacksquare

C. Experiment Details

Additional details regarding the experiment settings for the simulation described in Section V are as follows:

- The dynamics map used is $g : \mathbb{R}^3 \rightarrow \mathbb{R}^3$, as given by:

$$g(x) := x + x_{\text{odom}} + w, \quad w \sim \mathcal{N}(0, \Sigma_w),$$

for each $x, x_{\text{odom}} \in \mathbb{R}^3$, with $\Sigma_w \in \mathbb{R}^{3 \times 3}$ as one of the three choices given in 5, 6, and 7.

- The measurement map used is $h : \mathbb{R}^3 \times \mathbb{R}^2 \rightarrow \mathbb{R}^2$, given by:

$$h(x, f) := \begin{bmatrix} \cos x_3 & \sin x_3 \\ -\sin x_3 & \cos x_3 \end{bmatrix} \begin{bmatrix} f_1 - x_1 \\ f_2 - x_2 \end{bmatrix} + v, \quad v \sim \mathcal{N}(0, \Sigma_v),$$

for each $x := (x_1, x_2, x_3) \in \mathbb{R}^3$ and $f := (f_1, f_2) \in \mathbb{R}^2$, with $\Sigma_v \in \mathbb{R}^{2 \times 2}$ as one of the three choices given in 5, 6, and 7.

- The moving object pose map transform $g^o : \mathbb{R}^3 \times \mathbb{R}^{2n_{\text{of}}} \rightarrow \mathbb{R}^{2n_{\text{of}}}$ is given by:

$$f^c := \frac{1}{n_{\text{of}}} \sum_{j=1}^{n_{\text{of}}} f_j,$$

$$g^o(\xi, f_{\text{vec}})$$

$$\begin{aligned} &:= \text{vec} \left(\begin{bmatrix} \cos \xi_3 & -\sin \xi_3 \\ \sin \xi_3 & \cos \xi_3 \end{bmatrix} \right. \\ & \quad \left. \cdot \begin{bmatrix} f_1^1 - f_1^c & \dots & f_1^n - f_1^c \\ f_2^1 - f_2^c & \dots & f_2^n - f_2^c \end{bmatrix} \right. \\ & \quad \left. + \begin{bmatrix} f_1^c + \xi_1 \\ f_2^c + \xi_2 \end{bmatrix} \begin{bmatrix} 1 & \dots & 1 \end{bmatrix} \right), \end{aligned}$$

$$= \begin{bmatrix} (f_1^1 - f_1^c) \cos \xi_3 - (f_2^1 - f_2^c) \sin \xi_3 + f_1^c + \xi_1 \\ (f_2^1 - f_2^c) \cos \xi_3 - (f_1^1 - f_1^c) \sin \xi_3 + f_2^c + \xi_2 \\ \vdots \\ (f_1^n - f_1^c) \cos \xi_3 - (f_2^n - f_2^c) \sin \xi_3 + f_1^c + \xi_1 \\ (f_2^n - f_2^c) \cos \xi_3 - (f_1^n - f_1^c) \sin \xi_3 + f_2^c + \xi_2 \end{bmatrix}$$

for each ξ . Here, we have defined $f_{\text{vec}} := (f_1^1, f_2^1, \dots, f_1^n, f_2^n) \in \mathbb{R}^{2n}$, and defined the *vectorization operator* vec as follows: Given $A \in \mathbb{R}^{m \times n}$, we have $\text{vec}(A) := (A_{11}, \dots, A_{1n}, \dots, A_{m1}, \dots, A_{mn}) \in \mathbb{R}^{mn}$.

- For the moving pose augmentation step, we use $\Sigma_{\xi} := 0.1 \cdot I_{2 \times 2}$ for all simulations. The SVD solution to Wahba’s problem is used to initialize all pose transformations from positions of each moving object feature observed at the initial time and at the current time.

- Due to the relatively smooth trajectories of this simulated scenario, the smoothing cost was omitted.
- As discussed in the main body of this tutorial, past moving object features and poses are dropped from the optimization window to ease the computational burden of the dynamic EKF SLAM algorithm at future timesteps. Note that, in real-life autonomous navigation tasks, dropping such poses and features far in the past would not severely impact the pose and feature estimation capabilities of the ego robot in the present and near future.